Electronic Supplementary Material (ESI) for Dalton Transactions.
This journal is © The Royal Society of Chemistry 2021

Supplementary Information

Intercluster exchanges leading to hydride-centered bimetallic clusters: a multi-NMR, X-ray crystallographic, and DFT Study

Yu-Jie Zhong,[a] Jian-Hong Liao,[a] Tzu-Hao Chiu,[a] Ying-Yann Wu,[b] Samia Kahlal,[c] Michael J. McGlinchey,[d] Jean-Yves Saillard [c] and C. W. Liu*[a]

[a] *Department of Chemistry, National Dong Hwa University, Hualien 974301, Taiwan, Republic of China. E-mail: chenwei@mail.ndhu.edu.tw*
[b] *Institute of Chemistry, Academia Sinica, Taipei 11528, Taiwan, Republic of China.*
[c] Univ Rennes, CNRS, ISCR-UMR 6226, F-35000 Rennes, France
[d] *UCD School of Chemistry, University College Dublin, Belfield, Dublin 4, Ireland*

Experimental Section

Materials and measurements. All organic solvents and chemicals were purchased from commercial sources and the solvents were purified by standard procedures.[1] All the reactions were carried out in oven-dried Schlenk glassware under an inert atmosphere of nitrogen. $[M(CH_3CN)_4](PF_6)$, M = Cu,[2] Ag;[2] and $NH_4[E_2P(O^iPr)_2]$, E = S,[3] Se,[4] were prepared by a slight modification of the literature procedure. ^1H, ^{109}Ag, ^{31}P, ^{77}Se and ^2H NMR spectra were recorded on Bruker AV-600 BBO probe, and Bruker Avance DPX-300 BBO probe spectrometers, respectively, operating at 599.95 MHz for ^1H, 46.07 MHz for ^2H, 121.49 and 242.86 MHz for ^{31}P, 57.24 and 114.42 MHz for ^{77}Se, and 27.918 MHz for ^{109}Ag. Chemical shifts (δ) and coupling constants (*J*) are reported in ppm and Hz, respectively. ESI-mass spectra were recorded on a Fison Quattro Bio-Q (Fisons Instruments, VG Biotech, U. K.). The elemental analysis (C, H, and S content) of the sample was determined by Elementar UNICUBE elemental analyzer.

Synthesis of $[Ag_7(H)\{S_2P(O^iPr)_2\}_6]$, 1. The synthetic procedure followed the literature preparation of $[Ag_7(H)\{S_2P(OEt)_2\}_6]$.[5] The diisopropyl dithiophosphate ligand, $[S_2P(O^iPr)_2]^-$, was used instead of $[S_2P(OEt)_2]^-$. $[Ag(CH_3CN)_4]PF_6$ (0.30 g, 0.54 mmol) and $NH_4[S_2P(O^iPr)_2]$ (0.119 g, 0.46 mmol) were dissolved in iced THF (50 mL) at -20°C. $NaBH_4$ (0.0046 g, 0.12 mmol) was added and the solution was stirred for 1 hour. The color of the solution changed from transparent to black. It was dried under vacuum and washed by CH_2Cl_2/DI-H_2O in order to remove the residual borohydride. The organic layer was collected and passed through an alumina column. The colorless eluent was collected and dried to yield $[Ag_7(H)\{S_2P(O^iPr)_2\}_6]$ (0.1955 g, 80.0%). $^{31}P\{^1H\}$ NMR (121.49 MHz, $CDCl_3$, δ, ppm): 107.8. ^1H NMR (300.13 MHz, $CDCl_3$, δ, ppm): 1.34 (d, $^1J_{HH}$ = 5 Hz, 72H, *CH*$_3$), 4.78 (m, 12H, *CH*), 6.22 (pseudo octet, $^1J_{AgH}$ = 39.5 Hz, 1H, *Ag*$_7$*H*).

Synthesis of $[Cu_7(H)\{S_2P(O^iPr)_2\}_6]$, 2. The synthetic procedure followed the literature preparation of $[Cu_7(H)\{S_2P(OEt)_2\}_6]$.[6] The diisopropyl dithiophosphate ligand, $[S_2P(O^iPr)_2]^-$, was used instead of $[S_2P(OEt)_2]^-$. $[Cu(CH_3CN)_4]PF_6$ (0.301 g, 0.80 mmol) and $NH_4[S_2P(O^iPr)_2]$ (0.160 g, 0.69 mmol) were dissolved in iced THF (50 mL) at -20°C. $NaBH_4$ (0.0046 g, 0.12 mmol) was added and the solution was stirred for 1 hour. The light-yellow solution was dried under vacuum and washed by CH_2Cl_2/DI-H_2O in order to remove the residual borohydride. The organic layer was collected and dried. The solid was dissolved in diethyl ether and filtered to remove $[Cu_8(H)\{S_2P(O^iPr)_2\}_6]PF_6$. The filtrate was dried and washed with *n*-hexane to yield $[Cu_7(H)\{S_2P(O^iPr)_2\}_6]$ (0.151 g, 72.8%). $^{31}P\{^1H\}$ NMR (121.49 MHz, $CDCl_3$, δ, ppm): 103.8. ^1H NMR (300.13 MHz, $CDCl_3$, δ, ppm): 1.35 (d, $^1J_{HH}$ = 5 Hz, 72H, *CH*$_3$), 3.56 (s, 1H, *Cu*$_7$*H*), 4.81 (m, 12H, *CH*).

Synthesis of $[Ag_7(H)\{Se_2P(O^iPr)_2\}_6]$, 3. The compound was prepared by the reported literature procedure.[5]

Synthesis of $[Cu_7(H)\{Se_2P(O^iPr)_2\}_6]$, 4. $[Cu(CH_3CN)_4]PF_6$ (0.301 g, 0.80 mmol) and $NH_4[Se_2P(O^iPr)_2]$ (0.225 g, 0.69 mmol) were dissolved in iced THF (50 mL) at -20°C. $NaBH_4$ (0.0046 g, 0.12 mmol) was added and the solution was stirred for 1 hour. The light-yellow solution was dried under vacuum and washed with CH_2Cl_2/DI-H_2O in order to remove the residual borohydride. The organic layer was collected and dried. The solid was dissolved in diethyl ether and filtered to remove $[Cu_8(H)\{Se_2P(O^iPr)_2\}_6]PF_6$. The filtrate was dried and washed with *n*-hexane to yield $[Cu_7(H)\{Se_2P(O^iPr)_2\}_6]$ (0.204 g, 74.5%). $^{31}P\{^1H\}$ NMR (121.49 MHz, $CDCl_3$, δ, ppm): 86.2 ($^1J_{PSe}$ = 654.2 Hz). ^{77}Se NMR (57.24 MHz, $CDCl_3$, δ, ppm): 27.6 (d, $^1J_{PSe}$ = 654.7 Hz). ^1H NMR (300.13 MHz, $CDCl_3$, δ, ppm): -0.21 (s, 1H, *Cu*$_7$*H*), 1.37 (d, $^1J_{HH}$ = 6 Hz, 72H, *CH*$_3$), 4.78 (m, 12H, *CH*).

Time-dependent NMR spectroscopy. $[Ag_7(H)\{S_2P(O^iPr)_2\}_6]$, **1**, (0.0244 g, 0.012 mmol) and $[Cu_7(H)\{S_2P(O^iPr)_2\}_6]$, **2**, (0.0207 g, 0.012 mmol) were placed in an NMR tube and, as soon as $CDCl_3$ was added, the tube was inserted into the NMR spectrometer. The spectra were recorded after 1, 10, 20, 40, and 60 minutes, respectively.

Concentration-dependent NMR spectroscopy.

Synthesis of $[Cu_xAg_{7-x}(H)\{S_2P(O^iPr)_2\}_6]$, 5. $[Ag_7(H)\{S_2P(O^iPr)_2\}_6]$ and $[Cu_7(H)\{S_2P(O^iPr)_2\}_6]$ were weighed, respectively, according to different molar ratios which Ag_7:Cu_7 were 6:1 (0.0244 g, 0.012 mmol; 0.0035 g, 0.002 mmol), 4:1 (0.0244 g, 0.012 mmol; 0.005 g, 0.003 mmol), 2:1 (0.0244 g, 0.012 mmol; 0.0104 g, 0.006 mmol), 1:1 (0.0244 g, 0.012 mmol; 0.0207 g, 0.012 mmol), 1:2 (0.0122 g, 0.006 mmol; 0.0207 g, 0.012 mmol), 1:4 (0.0061 g, 0.003 mmol; 0.0207 g, 0.012 mmol), and 1:6 (0.0041 g, 0.002 mmol; 0.0207 g, 0.012 mmol), and placed in the NMR tube. $CDCl_3$ was then added to dissolve both compounds, and the NMR spectrum of each mixture was recorded after one hour of mixing. $^{31}P\{^1H\}$ NMR (121.49 MHz, $CDCl_3$, δ, ppm): 103.9 (s, *Cu*$_7$*H*), 104.9 (s, *Cu*$_6$*AgH*), 105.2 (s, *Cu*$_5$*Ag*$_2$*H*), 104.53 (s, *Cu*$_4$*Ag*$_3$*H*), 105.7 (s, *Cu*$_3$*Ag*$_4$*H*), 106.4 (s, *Cu*$_2$*Ag*$_5$*H*), 107.5 (s, *CuAg*$_6$*H*), 108.8 (s, *Ag*$_7$*H*). Anal. calcd. for $C_{108}H_{255}Ag_2Cu_{19}O_{36}P_{18}S_{36}$·5($CDCl_3$) [crystal **5a**·5($CDCl_3$] : C, 23.13; H, 4.55; S, 19.67. Found: C, 22.97; H, 4.65; S, 19.71.

Synthesis of $[Cu_xAg_{7-x}(H)\{Se_2P(O^iPr)_2\}_6]$, 6. $[Ag_7(H)\{Se_2P(O^iPr)_2\}_6]$ and $[Cu_7(H)\{Se_2P(O^iPr)_2\}_6]$

were weighted, respectively, according to different molar ratios which Ag_7:Cu_7 were 6:1 (0.0312 g, 0.012 mmol; 0.0046 g, 0.002 mmol), 4:1 (0.0312 g, 0.012 mmol; 0.0069 g, 0.003 mmol), 2:1 (0.0312 g, 0.012 mmol; 0.0137 g, 0.006 mmol), 1:1 (0.0312 g, 0.012 mmol; 0.0275 g, 0.012 mmol), 1:2 (0.0156 g, 0.006 mmol; 0.0275 g, 0.012 mmol), 1:4 (0.0078 g, 0.003 mmol; 0.0275 g, 0.012 mmol), and 1:6 (0.0052 g, 0.002 mmol; 0.0275 g, 0.012 mmol), and added into the NMR tube. $CDCl_3$ was then added into the tube to dissolve both compounds. The NMR spectrum of each mixture was recorded respectively after one hour of mixing. $^{31}P\{^1H\}$ NMR (242.86 MHz, $CDCl_3$, δ, ppm, *J*, Hz): 83.2 ($^1J_{PSe}$ = 662.2 Hz, *Ag_7H*), 83.0 ($^1J_{PSe}$ = 661.3, *$CuAg_6H$*), 83.0 ($^1J_{PSe}$ = 661.3, *Cu_2Ag_5H*), 83.4 ($^1J_{PSe}$ = 660.2, *Cu_3Ag_4H*), 84.0 ($^1J_{PSe}$ = 658.8, *Cu_4Ag_3H*), 84.7 ($^1J_{PSe}$ = 656.5, *Cu_5Ag_2H*), 85.4 ($^1J_{PSe}$ = 655.8, *Cu_6AgH*), 86.3 ($^1J_{PSe}$ = 653.6, *Cu_7H*). ^{77}Se NMR (114.42 MHz, $CDCl_3$, δ, ppm, *J*, Hz): 27.4 (d, $^1J_{Pse}$ = 660.2, *Ag_7*), 28.4 (d, $^1J_{Pse}$ = 659.1, *$CuAg_6$*), 28.4 (d, $^1J_{Pse}$ = 659.1, *Cu_2Ag_5*), 28.7 (d, $^1J_{Pse}$ = 660.2, *Cu_3Ag_4*), 26.8 (d, $^1J_{Pse}$ = 647.6, *Cu_4Ag_3*), 26.2 (d, $^1J_{Pse}$ = 671.6, *Cu_5Ag_2*), 24.3 (d, $^1J_{Pse}$ = 656.8, *Cu_6Ag*), 25.3 (d, $^1J_{Pse}$ = 659.1, *Cu_7*). ^1H NMR (599.95 MHz, $CDCl_3$, δ, ppm, *J*, Hz): 4.744 (m, 12H, *CH*), 3.557 (pseudo octet of octets, $^1J_{1H\text{-}107Ag}$ = 36.0, $^1J_{1H\text{-}109Ag}$ = 41.4, *Ag_7H*), 3.391 (pseudo septet of septets, $^1J_{1H\text{-}107Ag}$ = 42.4, $^1J_{1H\text{-}109Ag}$ = 48.7, *$CuAg_6H$*), 3.175 (pseudo sextet of sextets, $^1J_{1H\text{-}107Ag}$ = 49.2, $^1J_{1H\text{-}109Ag}$ = 56.6, *Cu_2Ag_5H*), 2.881 (pseudo quintet of quintets, $^1J_{1H\text{-}107Ag}$ = 53.8, $^1J_{1H\text{-}109Ag}$ = 61.9, *Cu_3Ag_4H*), 2.567 (pseudo quartet of quartets, $^1J_{1H\text{-}107Ag}$ = 57.6, $^1J_{1H\text{-}109Ag}$ = 66.2, *Cu_4Ag_3H*), 1.890 (pseudo triplet of triplets, $^1J_{1H\text{-}107Ag}$ = 58.3, $^1J_{1H\text{-}109Ag}$ = 67.0, *Cu_5Ag_2H*, 1.345 (d, $^1J_{HH}$ = 6.3, 72H, *CH_3*), 1.203 (two doublets, $^1J_{1H\text{-}107Ag}$ = 69.8, $^1J_{1H\text{-}109Ag}$ = 80.2, *Cu_6AgH*), -0.2864 (s, *Cu_7H*). ^{109}Ag DEPT NMR (27.918 MHz, *d*-chloroform, δ, ppm, *J*, Hz): 1123.1 (d, $^1J_{1H\text{-}109Ag}$ = 39.1, *Ag_7H*), 1137.5 (d, $^1J_{1H\text{-}109Ag}$ = 45.9 Hz, *$CuAg_6H$*), 1154.8 (d, $^1J_{1H\text{-}109Ag}$ = 56.1, *Cu_2Ag_5H*), 1058.7 (d, $^1J_{1H\text{-}109Ag}$ = 62.4, *Cu_3Ag_4H*), 1138.7 (d, $^1J_{1H\text{-}109Ag}$ = 67.6, *Cu_4Ag_3H*), 1096.8 (d, $^1J_{1H\text{-}109Ag}$ = 67.1, *Cu_5Ag_2H*), 1036.7 (d, $^1J_{1H\text{-}109Ag}$ = 83.1, *Cu_6AgH*). The ratio between individual compounds in each reaction is listed in Table 2. ESI-MS (m/z): exp. 2395.9264 (calc. 2396.1057) for $[Cu_7(H)\{Se_2P(O^iPr)_2\}_6 + Ag^+]^+$; exp. 2439.9041 (calc. 2440.4273) for $[Cu_6Ag(H)\{Se_2P(O^iPr)_2\}_6 + Ag^+]^+$; exp. 2485.8776 (calc. 2485.8200) for $[Cu_5Ag_2(H)\{Se_2P(O^iPr)_2\}_6 + Ag^+]^+$; exp. 2529.8558 (calc. 2529.7873) for $[Cu_4Ag_3(H)\{Se_2P(O^iPr)_2\}_6 + Ag^+]^+$; exp. 2573.8346 (calc. 2573.8085) for $[Cu_3Ag_4(H)\{Se_2P(O^iPr)_2\}_6 + Ag^+]^+$; exp. 2617.8125 (calc. 2617.7392) for $[Cu_2Ag_5(H)\{Se_2P(O^iPr)_2\}_6 + Ag^+]^+$; exp. 2661.7883 (calc. 2661.6970) for $[CuAg_6(H)\{Se_2P(O^iPr)_2\}_6 + Ag^+]^+$; exp. 2706.9715 (calc. 2706.6930) for $[Ag_7(H)\{Se_2P(O^iPr)_2\}_6 + Ag^+]^+$. Anal. calcd. for $C_{36}H_{85}Ag_6CuO_{12}P_6Se_{12}\cdot(CDCl_3)$ [crystal **6a**$\cdot(CDCl_3)$] : C, 16.62; H, 3.28. Found: C, 16.43; H, 3.12.

X-ray crystallography. Single crystals suitable for X-ray diffraction analysis of **2**, **5a**, and **6a** were obtained by diffusing hexane into concentrated methanol solution at 4 °C. The single crystal was mounted on the tip of glass fiber coated in paratone oil, then frozen at 100 K. Data were collected on a Bruker APEX II CCD diffractometer using graphite mono-chromated Mo(K_α) radiation (λ = 0.71073 Å). Absorption corrections for the area detector were performed with SADABS[7] and the integration of raw data frames was performed with SAINT[8]. The structure was solved by direct methods and refined by least-squares against F^2 using the SHELXL-2018/3 package,[9] incorporated

in SHELXTL/PC V6.14.[10] All non-hydrogen atoms were refined anisotropically and the central hydride of each structure was refined freely. In structure **2**, two molecules were found in the asymmetric unit where one of the Cu_7 cores in tricapped tetrahedral geometry (Figure S31) was disordered at two orientations (7 x 2 = 14 sites) with equal occupancy (0.5:0.5). The other molecule has severe disorder in the Cu_7 core in which the central tetrahedral core constitued by four Cu atoms were disordered at eight sites with total occupancy of 4. The remaining three capping Cu atoms were disordered at eight sites with total occupancy of 3. Thus the later Cu_7 core were disordered at 16 sites (8 + 8). The crystal **5a** was obtained from the reaction product of Ag_7 (**1**) and Cu_7 (**2**) in 1:6 molar ratio. A cocrystal of $Cu_7(H)\{S_2P(O^iPr)_2\}_6$ and $Cu_6Ag(H)\{S_2P(O^iPr)_2\}_6$ with a stoichometric ratio of 2:1 was solved. Both metal cores of tricapped tetrahedron showed similar disorder with mutiple orientations (8 + 8 = 16 sites). The Ag atoms in Cu_6Ag core were found to be located on the central tetrahedron only (Figure S32), and the Ag was disordered at the central tetrahedron (inner 8 sites). The crystal **6a** was obtained from the reaction product of Ag_7 (**3**) and Cu_7 (**4**) in 1:6 molar ratio. The $CuAg_6$ core of tricapped tetrahedron is disordered at two orientations (7 x 2 = 14 sites) with equal occupancy (0.5:0.5). The Cu atom in $CuAg_6$ core was found to be located on the capping positions only (Figure S33), where the Cu disordered at 6 capping positions (3 x 2) are in equal occupancy (0.16667). CCDC 2051209-2051211 contains the supplementary crystallographic data for compounds **2**, **5a**, and **6a** in this article. These data can be obtained free of charge from The Cambridge Crystallographic Data Centre via www. ccdc.cam.ac.uk/data_request/cif.

ESI-MS measurements. Mass spectra of all samples were recorded on a Bruker maXis ESI-QTOF quadrupole time-of-flight tandem mass spectrometer. Mass spectrometry was calibrated with a tuning mix. The operating parameters of the electrospray ionization interface (ESI) in positive mode were: capillary voltage, 4000 V; end plate offset, 500 V; dry gas temperature, 200 °C (N_2); dry gas flow, 4 L/min; and nebulizer pressure, 0.2 bar. Nitrogen was used as the nebulizing gas. The mass range scanned from 50 m/z to 6000 m/z.

Computational details. Geometry optimizations were performed by DFT calculations with the Gaussian 16 package,[11] using the BP86 functional,[12-13] together with Grimme's empirical DFT-D3 corrections for dispersion forces[14] and the all-electron Def2-TZVP set from EMSL Basis Set Exchange Library.[15] All the optimized geometries were characterized as true minima on their potential energy surface by harmonic vibrational analysis. The ^1H NMR chemical shifts were computed, according to the GIAO method,[16] as implemented in Gaussian 16.

References

S1. D. D. Perrin and W. L. F. Armarego, Purification of laboratory chemicals. 3rd Edition, Pergamon Press, Oxford, 1988.

S2. G. J. Kubas, B. Monzyk, A. L. Crumbliss, *Inorg. Synth.*, 1979, **19**, 90-92.

S3. V. P. Wystrach, E. O. Hook and G. L. M. Christopher, *J. Org. Chem.*, 1956, **21**, 705-707.

S4. V. Krishnan and R. A. Zingaro, *Inorg. Chem.*, 1969, **8**, 2337-2340.

S5. C. W. Liu, Y.-R. Lin, C.-S. Fang, C. Latouche, S. Kahlal and J.-Y. Saillard, *Inorg. Chem.*, 2013, **52**, 2070-2077.
S6. C. Latouche, S. Kahlal, Y.-R. Lin, J.-H. Liao, E. Furet, C. W. Liu and J.-Y. Saillard, *Inorg. Chem.*, 2013, **52**, 13253-13262.
S7. SADABS, version 2014-11.0, Bruker Area Detector Absorption Corrections, Bruker AXS Inc., Madison, Wisconsin, 2014.
S8. SAINT, V8.30A, Software for the CCD detector system, Bruker Analytical, Madison, Wisconsin, 2012.
S9. G. M. Sheldrick, *Acta. Cryst.*, 2008, **A64**, 112-122.
S10. SHELXTL, version 6.14., Bruker AXS Inc., Madison, Wisconsin, USA, 2003.
S11. Gaussian 16, Revision C.01, M. J. Frisch, G. W. Trucks, H. B. Schlegel, G. E. Scuseria, M. A. Robb, J. R. Cheeseman, G. Scalmani, V. Barone, G. A. Petersson, H. Nakatsuji, X. Li, M. Caricato, A. V. Marenich, J. Bloino, B. G. Janesko, R. Gomperts, B. Mennucci, H. P. Hratchian, J. V. Ortiz, A. F. Izmaylov, J. L. Sonnenberg, D. Williams-Young, F. Ding, F. Lipparini, F. Egidi, J. Goings, B. Peng, A. Petrone, T. Henderson, D. Ranasinghe, V. G. Zakrzewski, J. Gao, N. Rega, G. Zheng, W. Liang, M. Hada, M. Ehara, K. Toyota, R. Fukuda, J. Hasegawa, M. Ishida, T. Nakajima, Y. Honda, O. Kitao, H. Nakai, T. Vreven, K. Throssell, J. A. Montgomery Jr., J. E. Peralta, F. Ogliaro, M. J. Bearpark, J. J. Heyd, E. N. Brothers, K. N. Kudin, V. N. Staroverov, T. A. Keith, R. Kobayashi, J. Normand, K. Raghavachari, A. P. Rendell, J. C. Burant, S. S. Iyengar, J. Tomasi, M. Cossi, J. M. Millam, M. Klene, C. Adamo, R. Cammi, J. W. Ochterski, R. L. Martin, K. Morokuma, O. Farkas, J. B. Foresman and D. J. Fox, Gaussian, Inc., Wallingford CT, 2016.
S12. A. D. Becke, *Phys. Rev. A*, 1988, **38**, 3098-3100.
S13. J. P. Perdew, *Phys. Rev. B*, 1986, **33**, 8822-8824.
S14. S. Grimme, S. Ehrlich and L. J. Goerigk, *Comp. Chem.*, 2011, **32**, 1456-1465.
S15. F. Weigend and R. Ahlrichs, *Phys. Chem. Chem. Phys.*, 2005, **7**, 3297-3305.
S16. K. Wolinski, J. F. Hilton and P. Pulay, *J. Am. Chem. Soc*., 1990, **112**, 8251-8260.

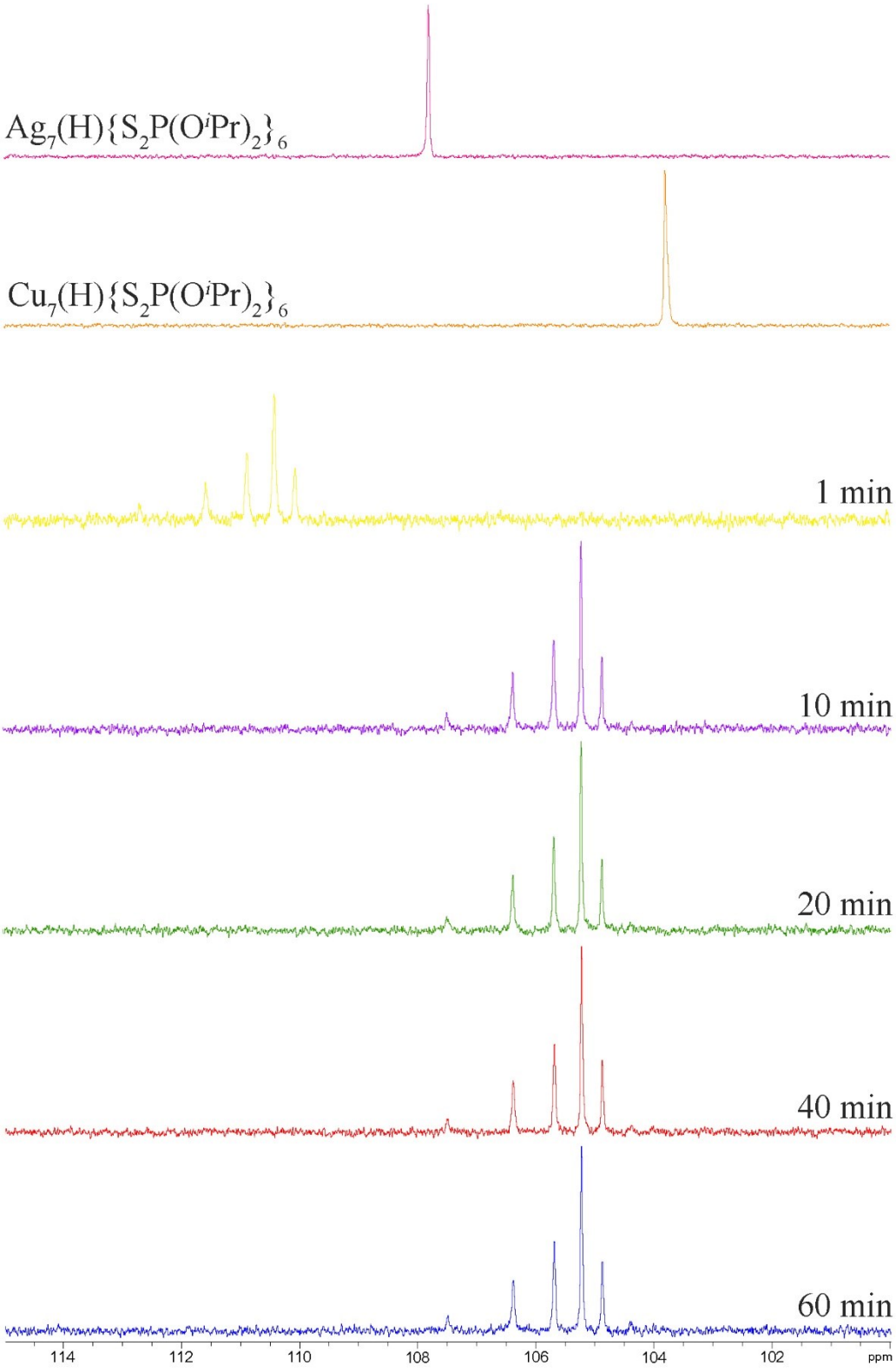

Figure S1. Time-dependent ^{31}P NMR (121.49 MHz) spectra of the reaction of compounds **1** and **2** in equal molar ratio.

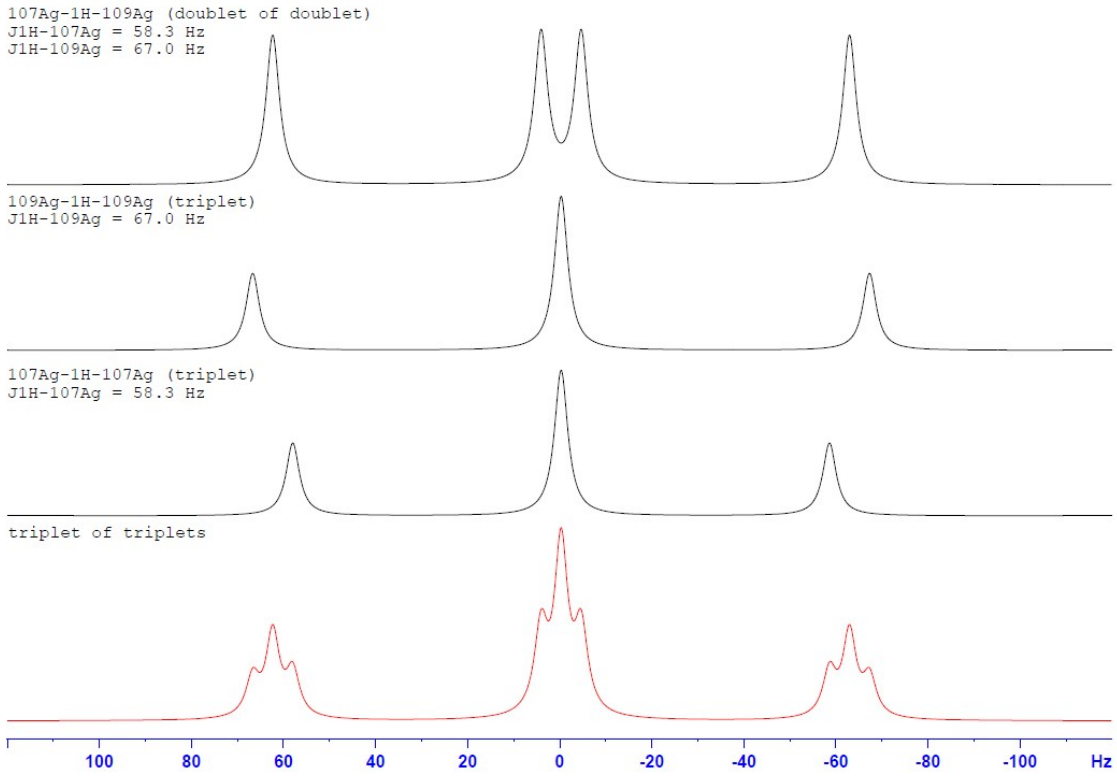

Figure S2. The deconvolution of coupling patterns in ^{1}H NMR spectrum, where the three combinations are ^{107}Ag-^{109}Ag, ^{109}Ag-^{109}Ag, and ^{107}Ag-^{107}Ag in $Cu_5Ag_2(H)\{Se_2P(O^iPr)_2\}_6$ (**6**).

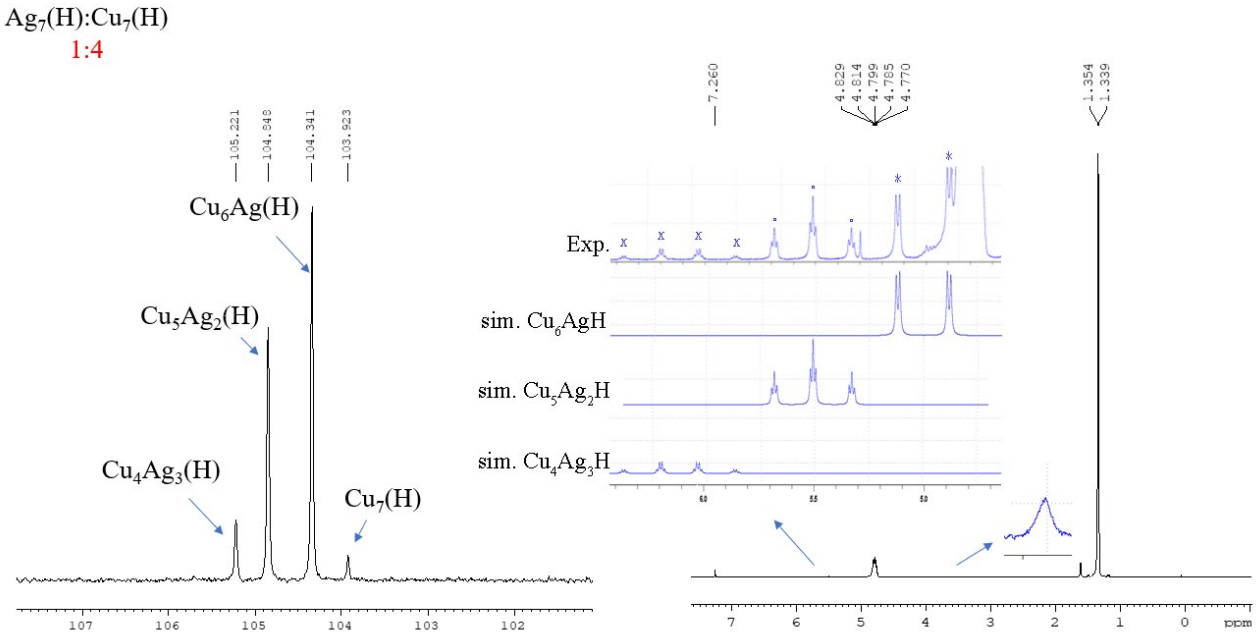

Figure S3. ^{31}P{^{1}H} (left) and ^{1}H (right) NMR spectra from the reaction of $Ag_7(H)\{S_2P(O^iPr)_2\}_6$ (**1**) and $Cu_7(H)\{S_2P(O^iPr)_2\}_6$ (**2**) in a 1:4 molar ratio. The inset spectra from top to bottom were experimental and simulation spectra of $Cu_6Ag(H)\{S_2P(O^iPr)_2\}_6$, $Cu_5Ag_2(H)\{S_2P(O^iPr)_2\}_6$, and $Cu_4Ag_3(H)\{S_2P(O^iPr)_2\}_6$, respectively.

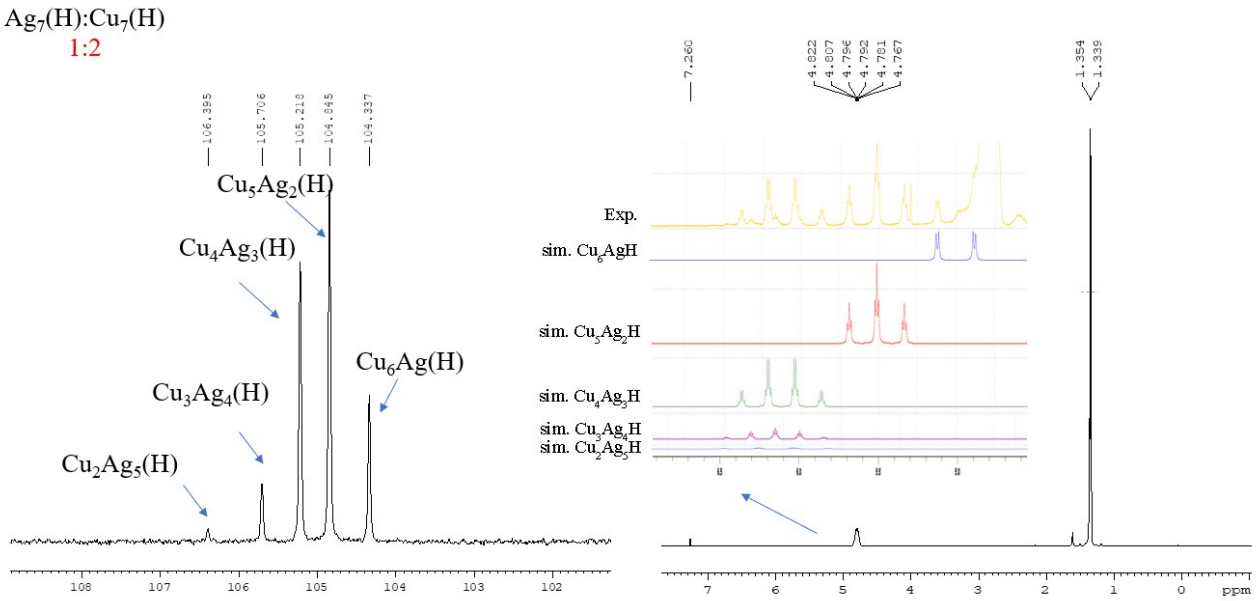

Figure S4. $^{31}P\{^{1}H\}$ (left) and ^{1}H (right) NMR spectra from the reaction of $Ag_7(H)\{S_2P(O^iPr)_2\}_6$ (**1**) and $Cu_7(H)\{S_2P(O^iPr)_2\}_6$ (**2**) in a 1:2 molar ratio. The inset spectra from top to bottom were experimental and simulation spectra of $Cu_6Ag(H)\{S_2P(O^iPr)_2\}_6$, $Cu_5Ag_2(H)\{S_2P(O^iPr)_2\}_6$, $Cu_4Ag_3(H)\{S_2P(O^iPr)_2\}_6$, $Cu_3Ag_4(H)\{S_2P(O^iPr)_2\}_6$, and $Cu_2Ag_5(H)\{S_2P(O^iPr)_2\}_6$, respectively.

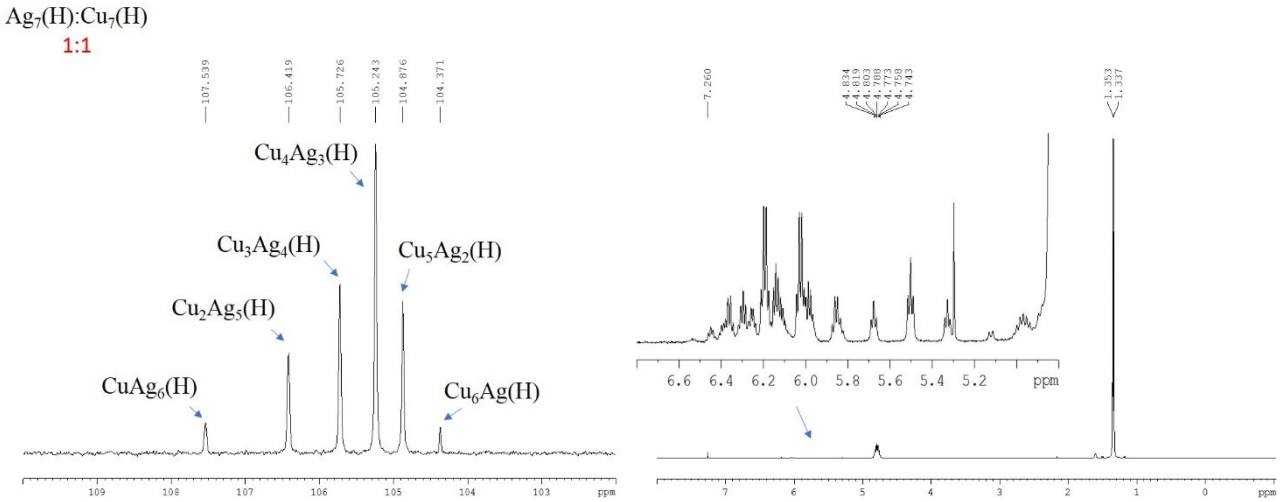

Figure S5. $^{31}P\{^{1}H\}$ (left) and ^{1}H (right) NMR spectra from the reaction of $Ag_7(H)\{S_2P(O^iPr)_2\}_6$ (**1**) and $Cu_7(H)\{S_2P(O^iPr)_2\}_6$ (**2**) with molar ratio 1:1.

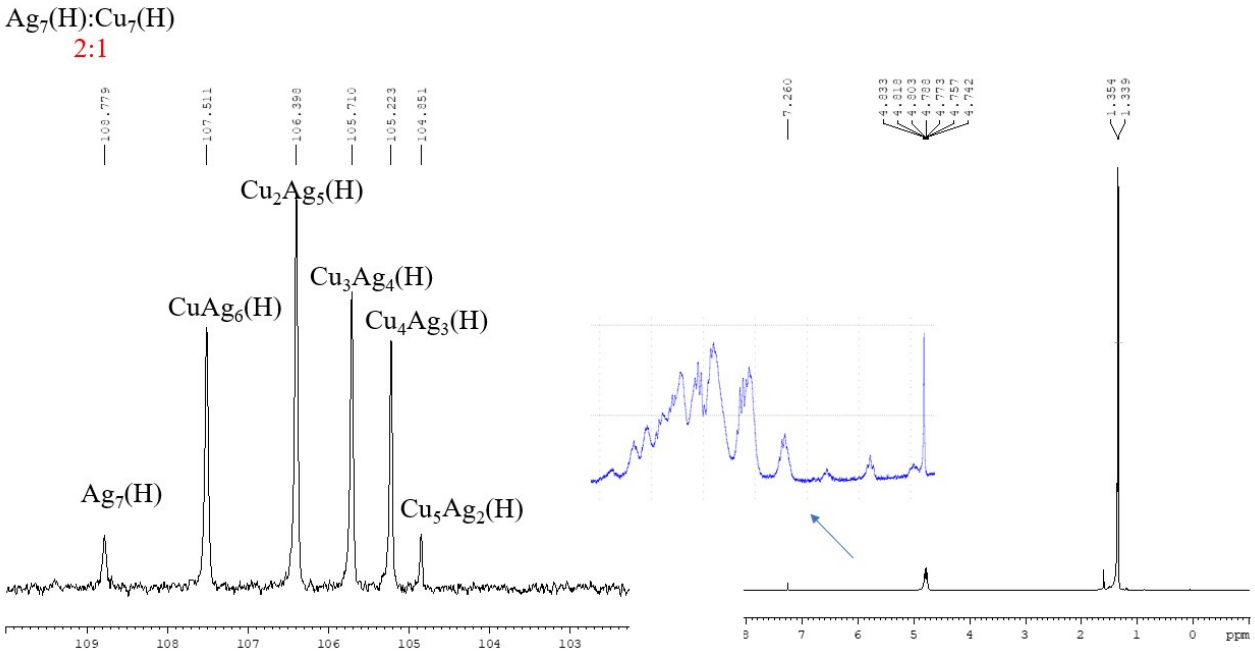

Figure S6. $^{31}P\{^{1}H\}$ (left) and ^{1}H (right) NMR spectra from the reaction of $Ag_7(H)\{S_2P(O^iPr)_2\}_6$ (**1**) and $Cu_7(H)\{S_2P(O^iPr)_2\}_6$ (**2**) with molar ratio 2:1.

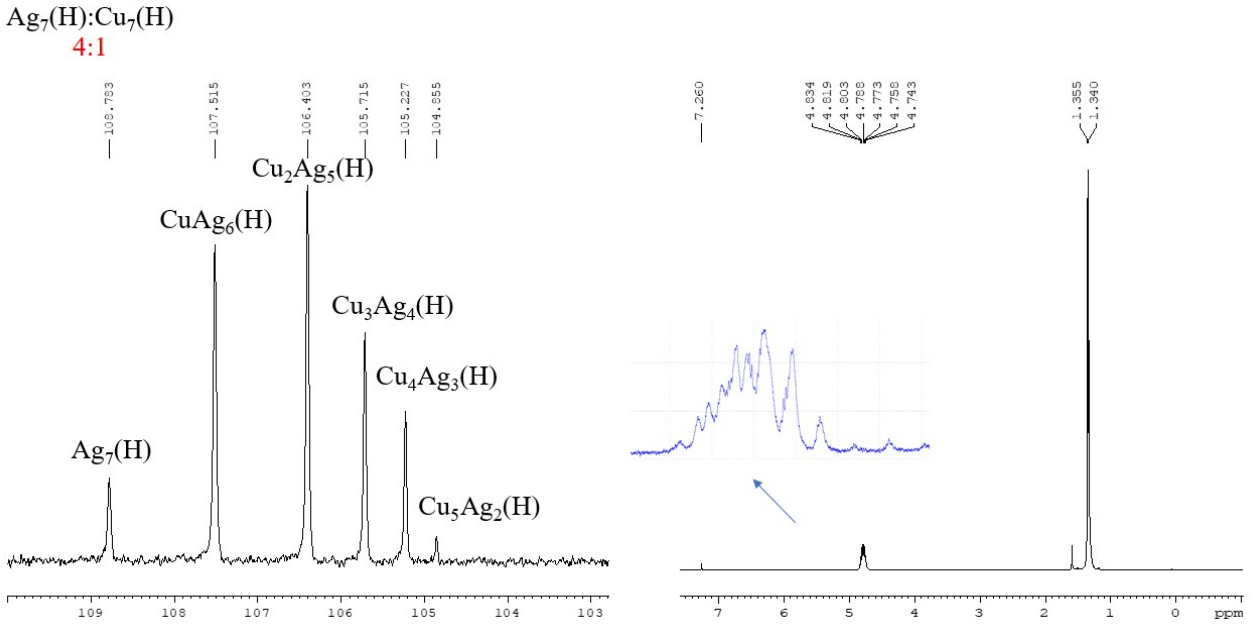

Figure S7. $^{31}P\{^{1}H\}$ (left) and ^{1}H (right) NMR spectra from the reaction of $Ag_7(H)\{S_2P(O^iPr)_2\}_6$ (**1**) and $Cu_7(H)\{S_2P(O^iPr)_2\}_6$ (**2**) in a 4:1 molar ratio.

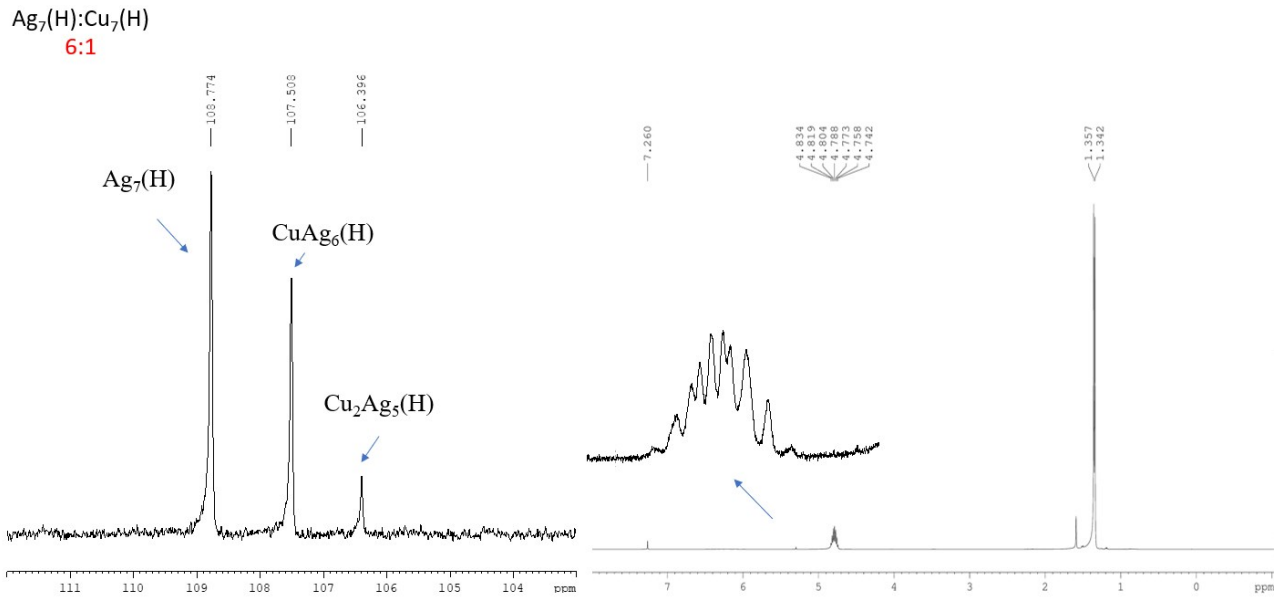

Figure S8. $^{31}P\{^{1}H\}$ (left) and ^{1}H (right) NMR spectra from the reaction of $Ag_7(H)\{S_2P(O^iPr)_2\}_6$ (**1**) and $Cu_7(H)\{S_2P(O^iPr)_2\}_6$ (**2**) in a 6:1 molar ratio.

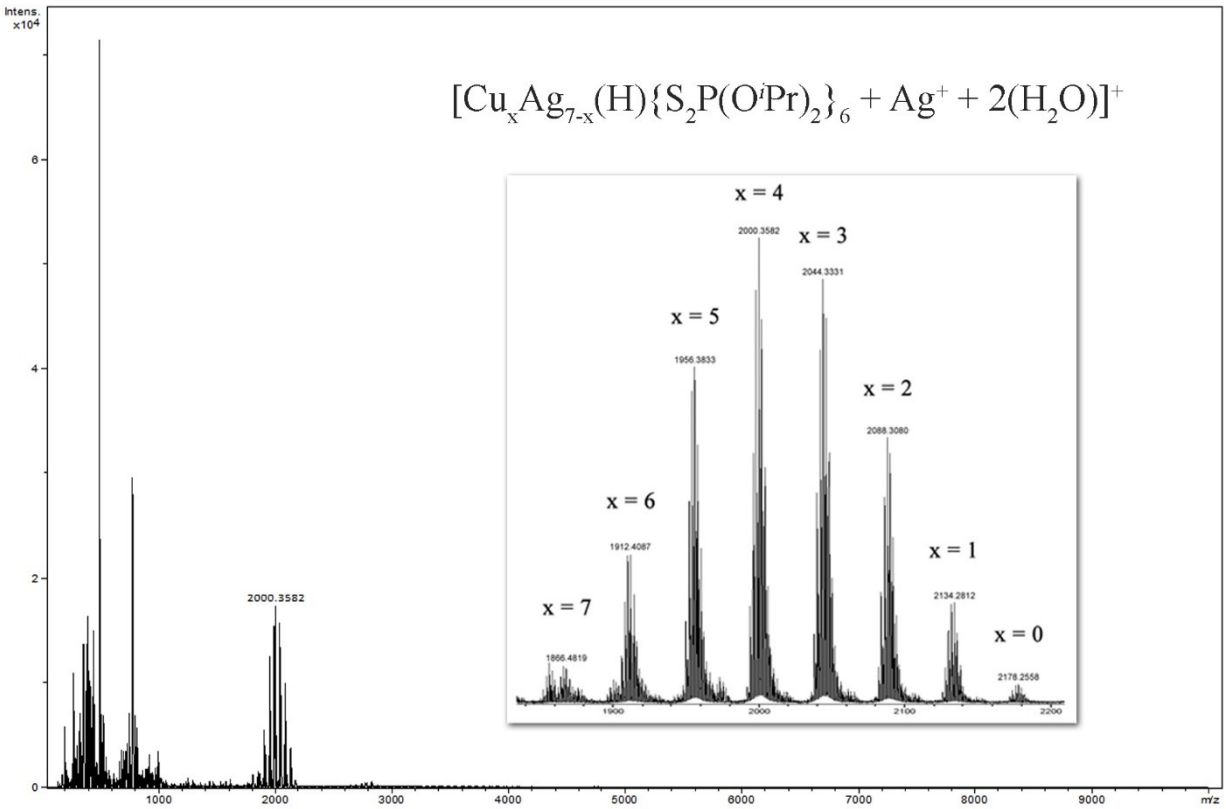

Figure S9. The positive-mode ESI mass spectrum of **5**.

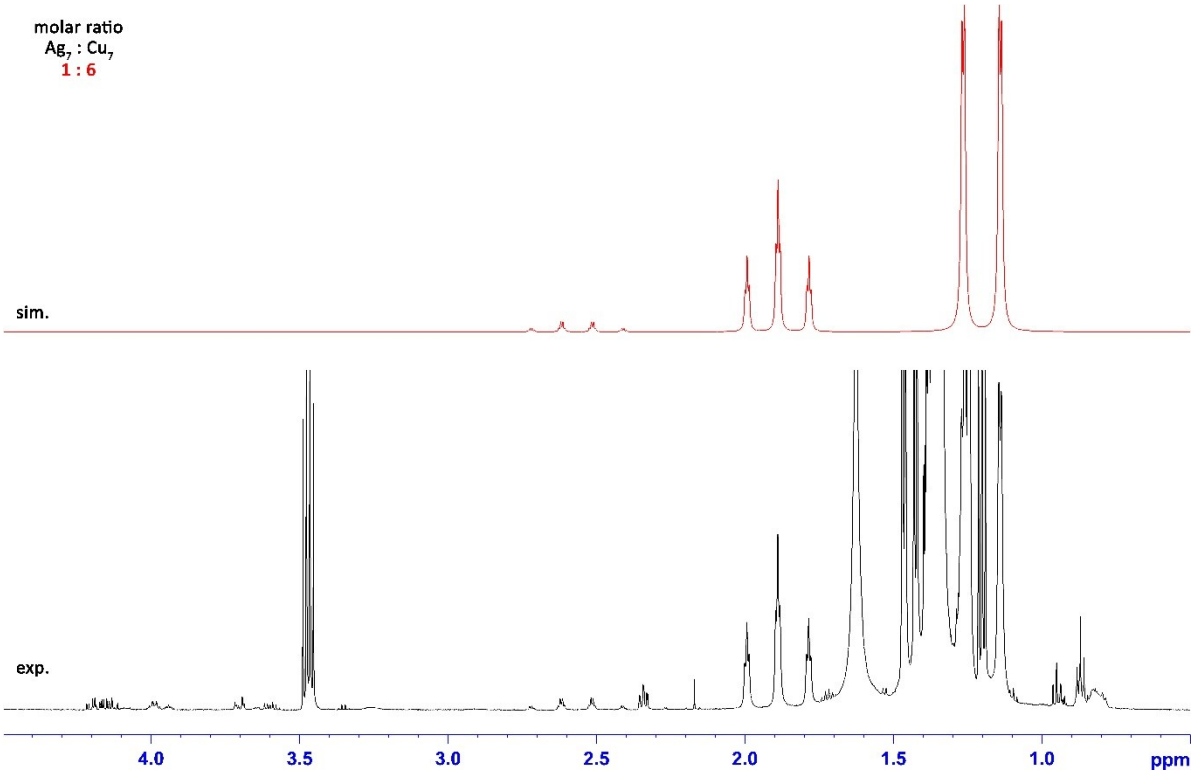

Figure S10. The simulation (up) and experimental (bottom) ^{1}H spectra of the products from the reaction of $Ag_7(H)\{Se_2P(O^iPr)_2\}_6$ (**3**) and $Cu_7(H)\{Se_2P(O^iPr)_2\}_6$ (**4**) in a 1:6 molar ratio.

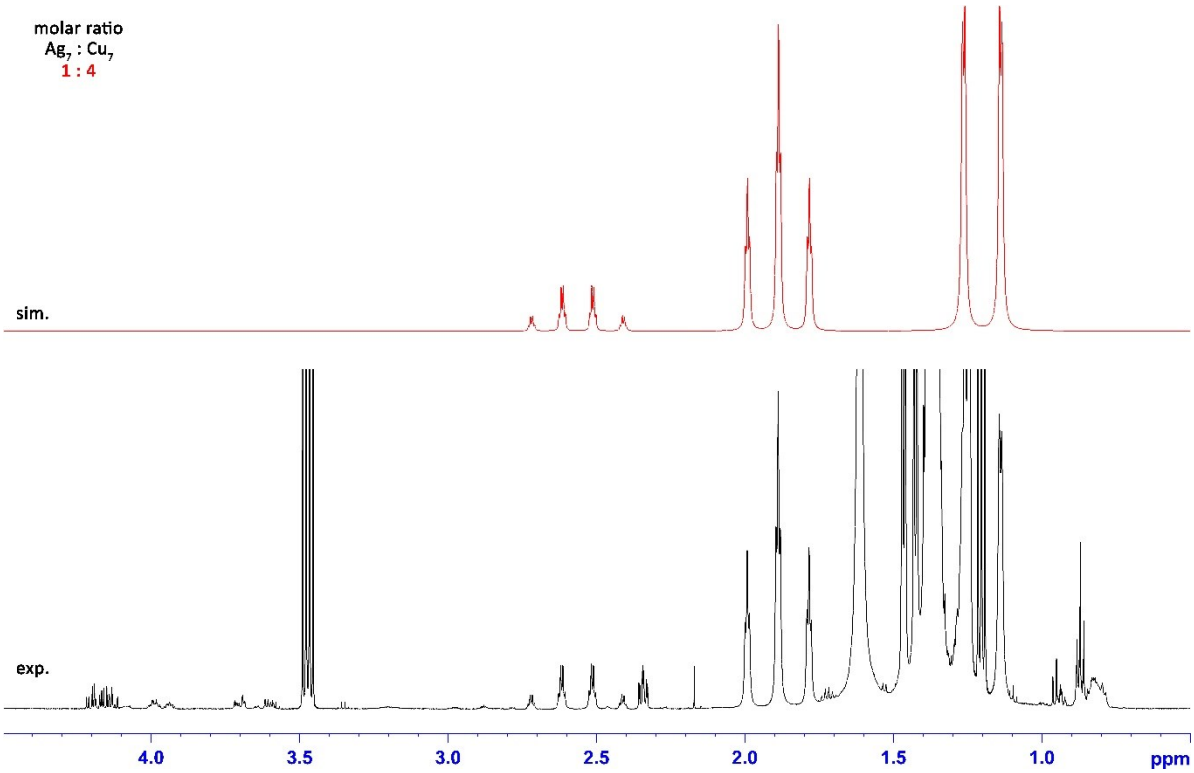

Figure S11. The simulation (up) and experimental (bottom) ^{1}H spectra of the products from the reaction of $Ag_7(H)\{Se_2P(O^iPr)_2\}_6$ (**3**) and $Cu_7(H)\{Se_2P(O^iPr)_2\}_6$ (**4**) in 1:4 molar ratio.

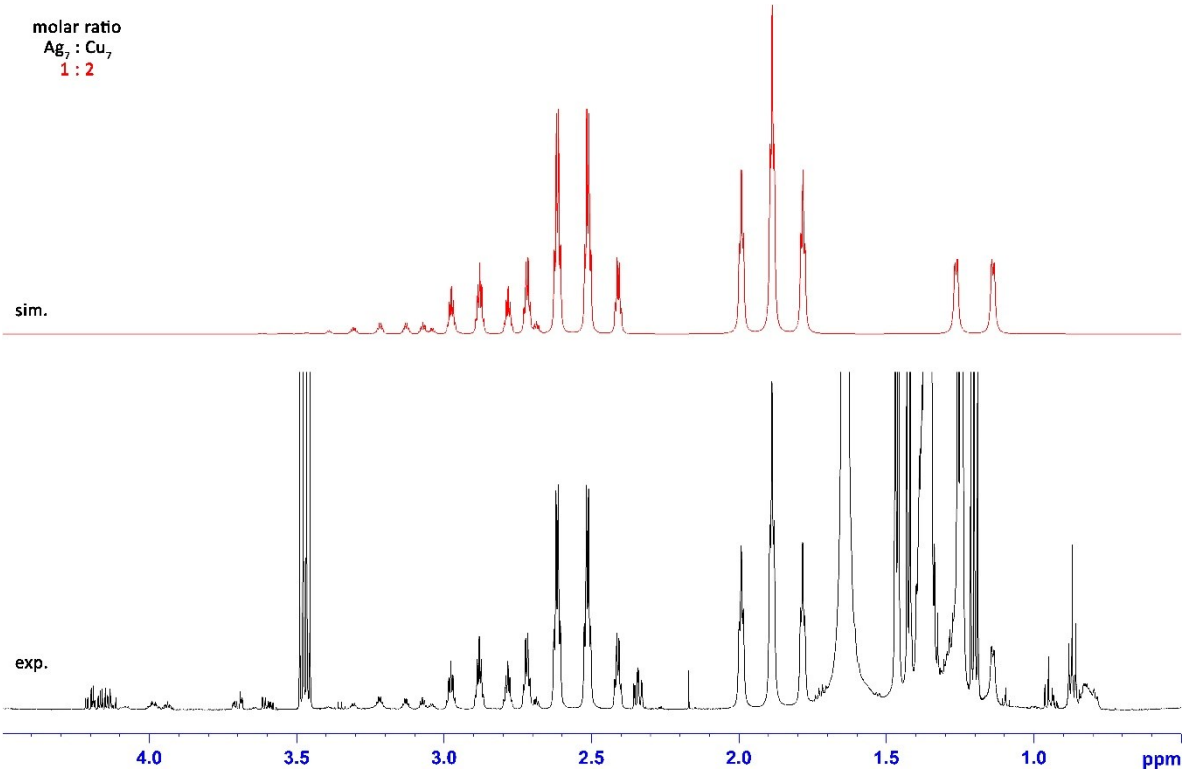

Figure S12. The simulation (up) and experimental (bottom) ^{1}H spectra of the products from the reaction of $Ag_7(H)\{Se_2P(O^iPr)_2\}_6$ (**3**) and $Cu_7(H)\{Se_2P(O^iPr)_2\}_6$ (**4**) with molar ratio of 1:2.

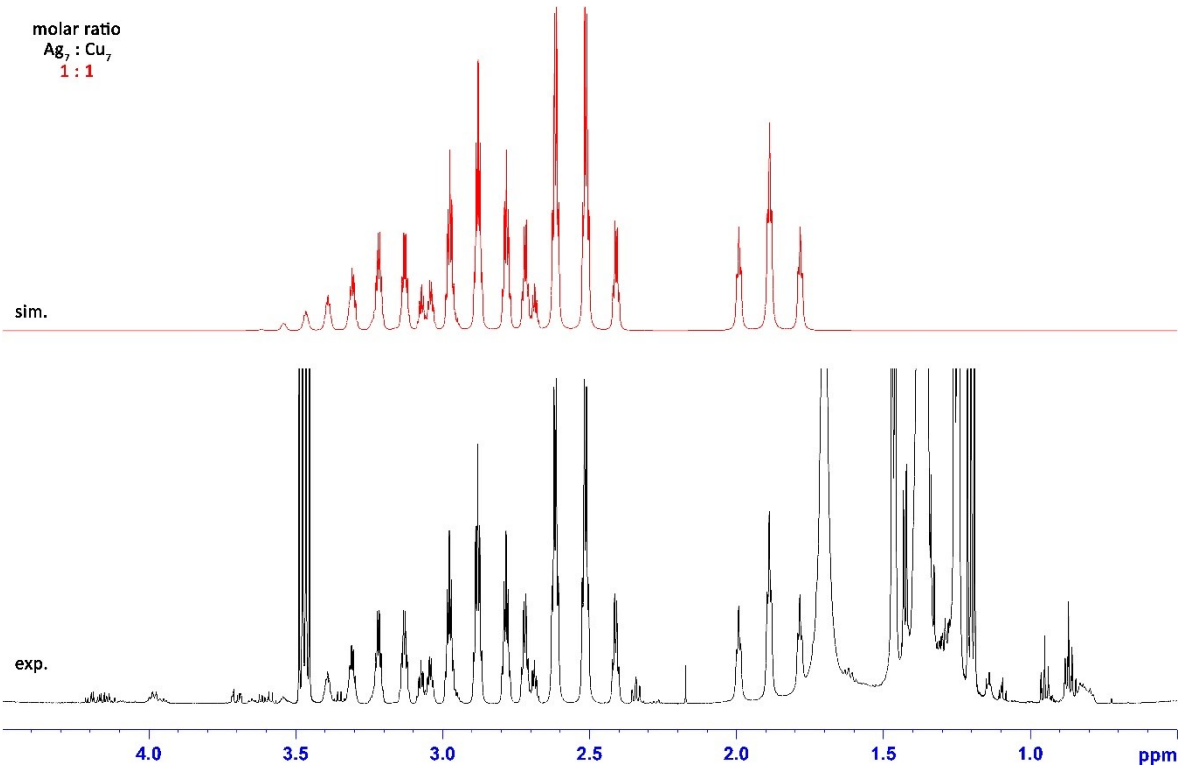

Figure S13. The simulation (up) and experimental (bottom) ^{1}H spectra of the products from the reaction of $Ag_7(H)\{Se_2P(O^iPr)_2\}_6$ (**3**) and $Cu_7(H)\{Se_2P(O^iPr)_2\}_6$ (**4**) with molar ratio of 1:1.

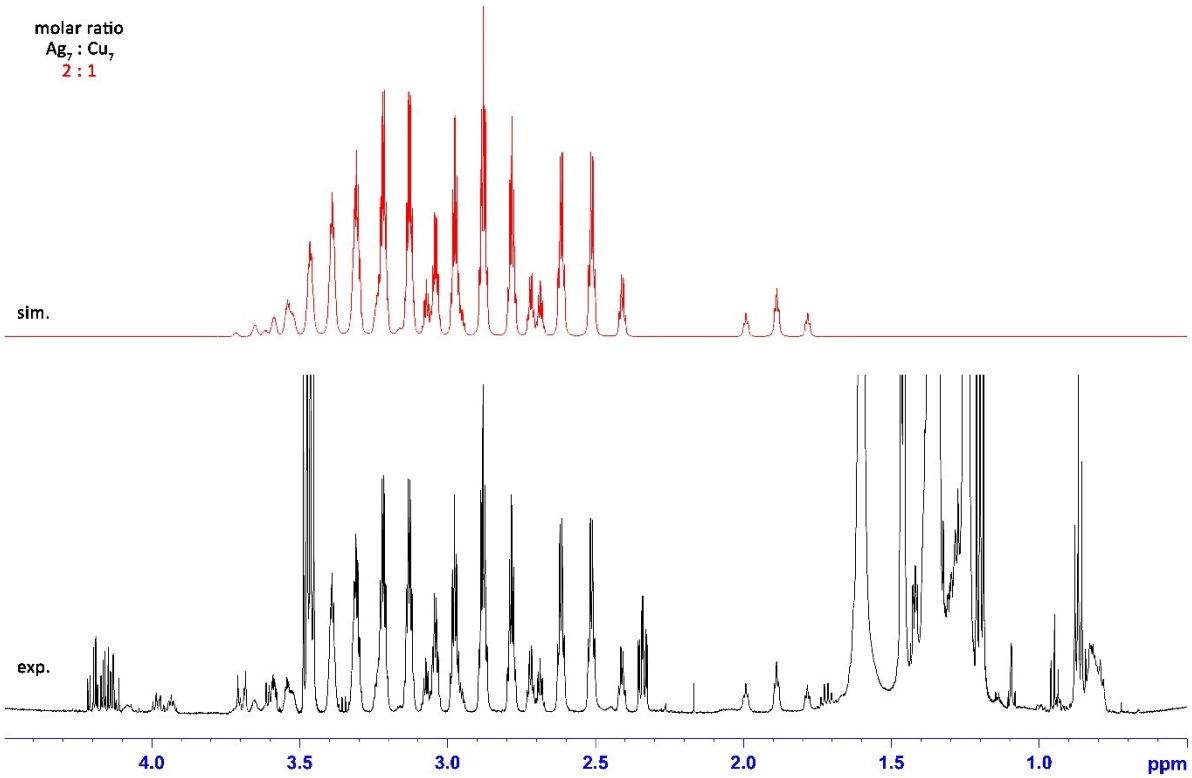

Figure S14. The simulation (up) and experimental (bottom) ^{1}H spectra of the products from the reaction of $Ag_7(H)\{Se_2P(O^iPr)_2\}_6$ (**3**) and $Cu_7(H)\{Se_2P(O^iPr)_2\}_6$ (**4**) with molar ratio of 2:1.

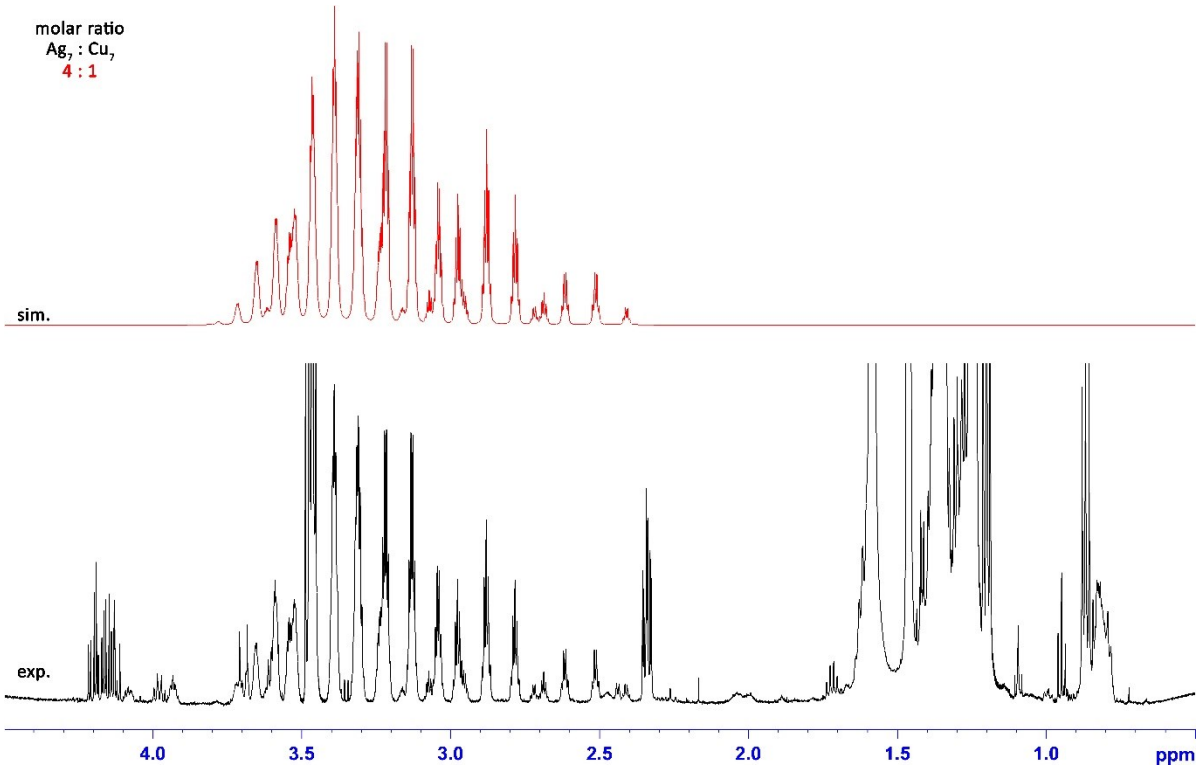

Figure S15. The simulation (up) and experimental (bottom) ^{1}H spectra of the products from the reaction of $Ag_7(H)\{Se_2P(O^iPr)_2\}_6$ (**3**) and $Cu_7(H)\{Se_2P(O^iPr)_2\}_6$ (**4**) with molar ratio of 4:1.

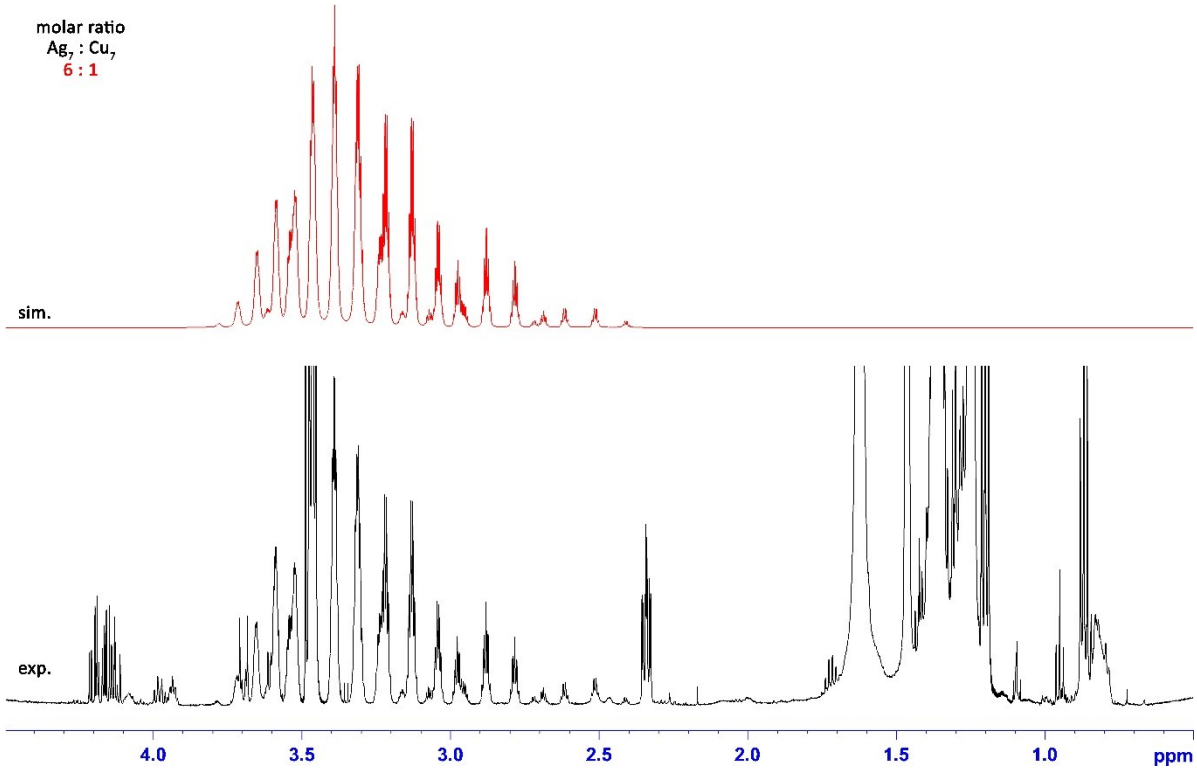

Figure S16. The simulation (up) and experimental (bottom) ^{1}H spectra of the products from the reaction of $Ag_7(H)\{Se_2P(O^iPr)_2\}_6$ (**3**) and $Cu_7(H)\{Se_2P(O^iPr)_2\}_6$ (**4**) with molar ratio of 6:1.

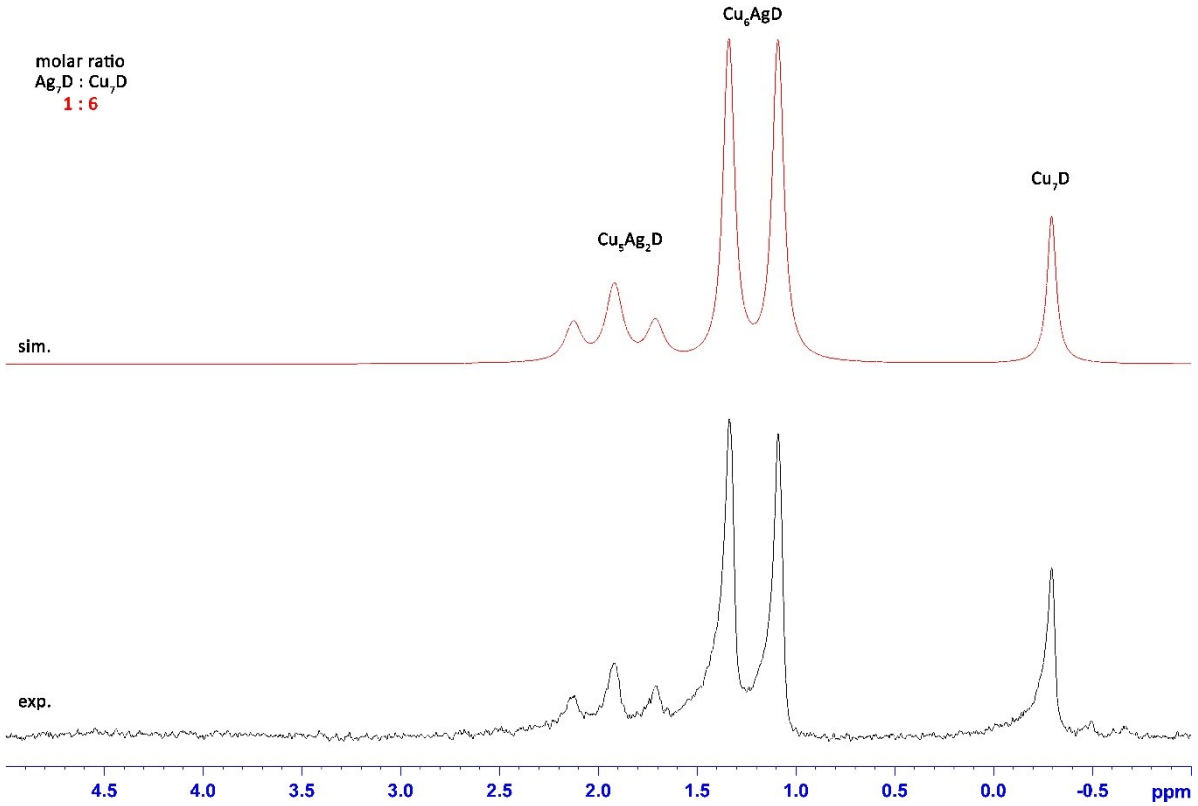

Figure S17. ^{2}H NMR spectrum of the products from the reaction of $Ag_7(D)\{Se_2P(O^iPr)_2\}_6$ (**3$_D$**) and $Cu_7(D)\{Se_2P(O^iPr)_2\}_6$ (**4$_D$**) with molar ratio of 1:6.

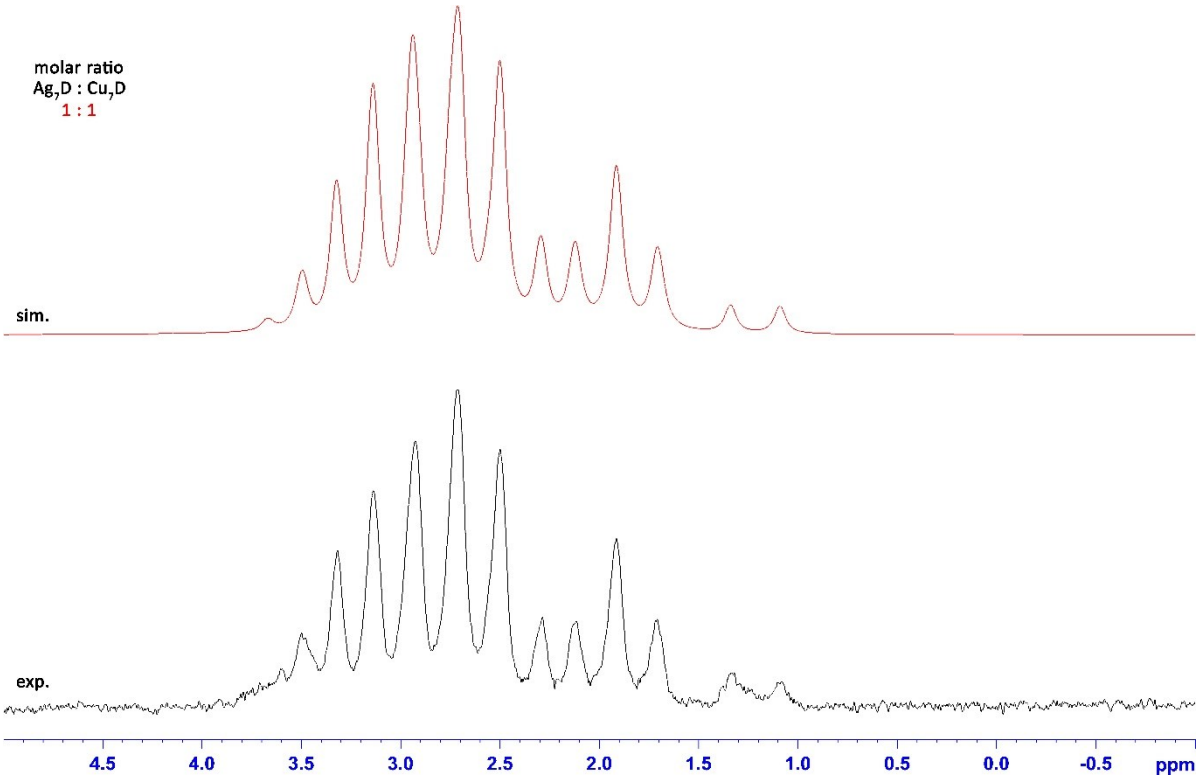

Figure S18. ^{2}H NMR spectrum of the products from the reaction of $Ag_7(D)\{Se_2P(O^iPr)_2\}_6$ (**3$_D$**) and $Cu_7(D)\{Se_2P(O^iPr)_2\}_6$ (**4$_D$**) with molar ratio of 1:1.

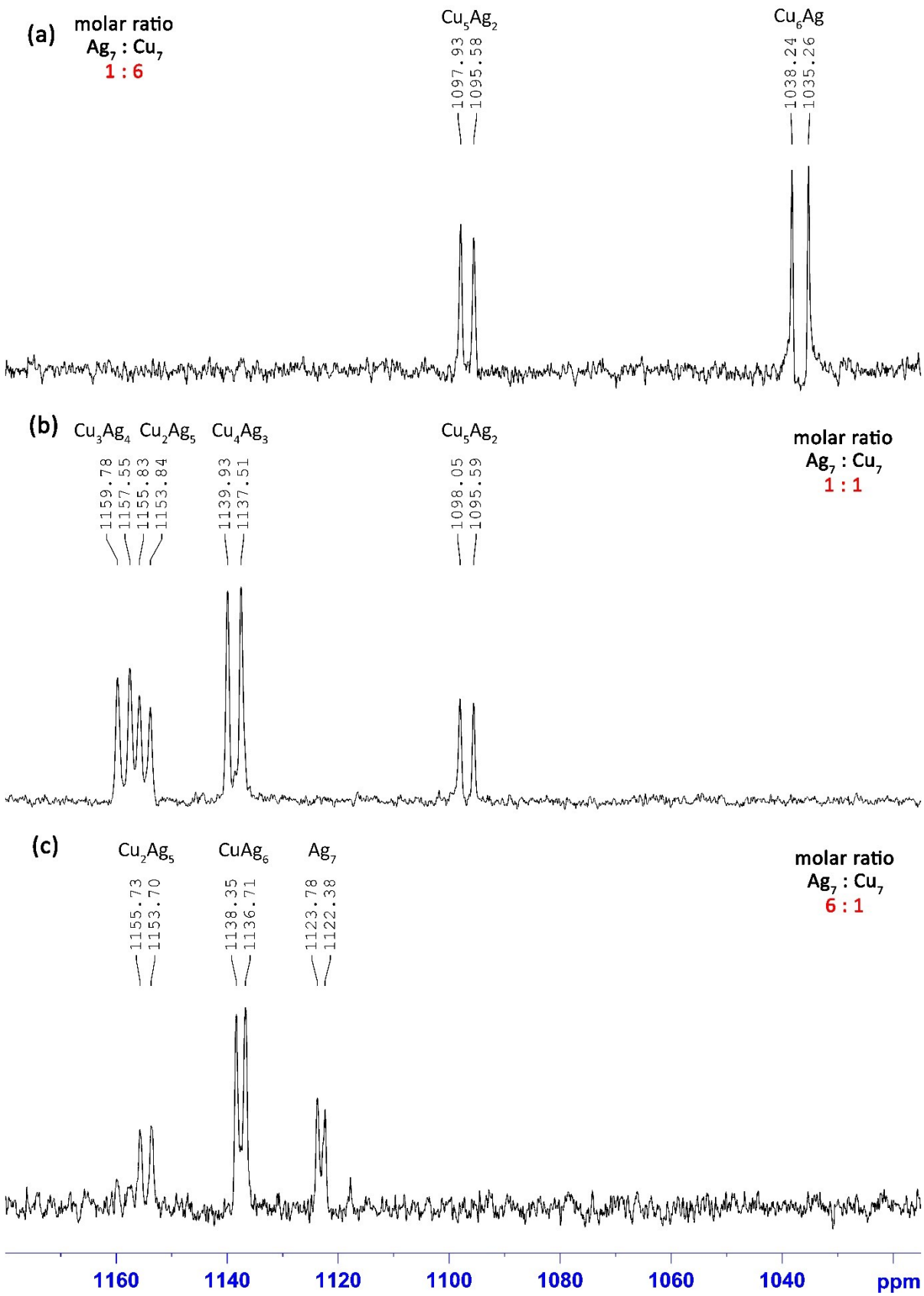

Figure S19. ^{109}Ag DEPT NMR spectra of (a) the products from the reaction of $Ag_7(H)\{Se_2P(O^iPr)_2\}_6$ (**3**) and $Cu_7(H)\{Se_2P(O^iPr)_2\}_6$ (**4**) in a 1:6, (b) 1:1, and (c) 6:1 molar ratio, respectively.

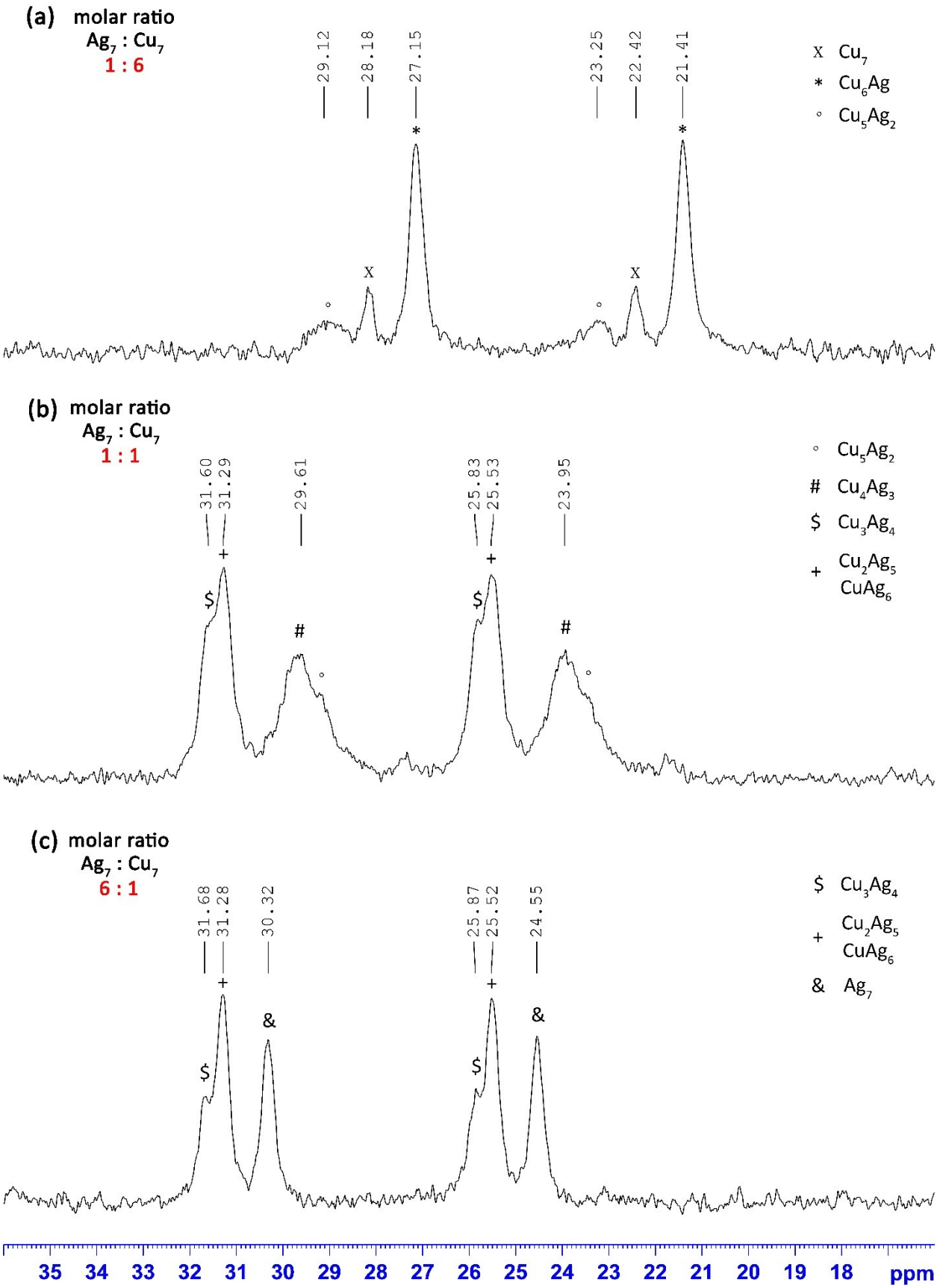

Figure S20. ^{77}Se NMR spectra of the products from the reaction of $Ag_7(H)\{Se_2P(O^iPr)_2\}_6$ (**3**) and $Cu_7(H)\{Se_2P(O^iPr)_2\}_6$ (**4**) in (a) 1:6, (b) 1:1, and (c) 6:1 molar ratio, respectively.

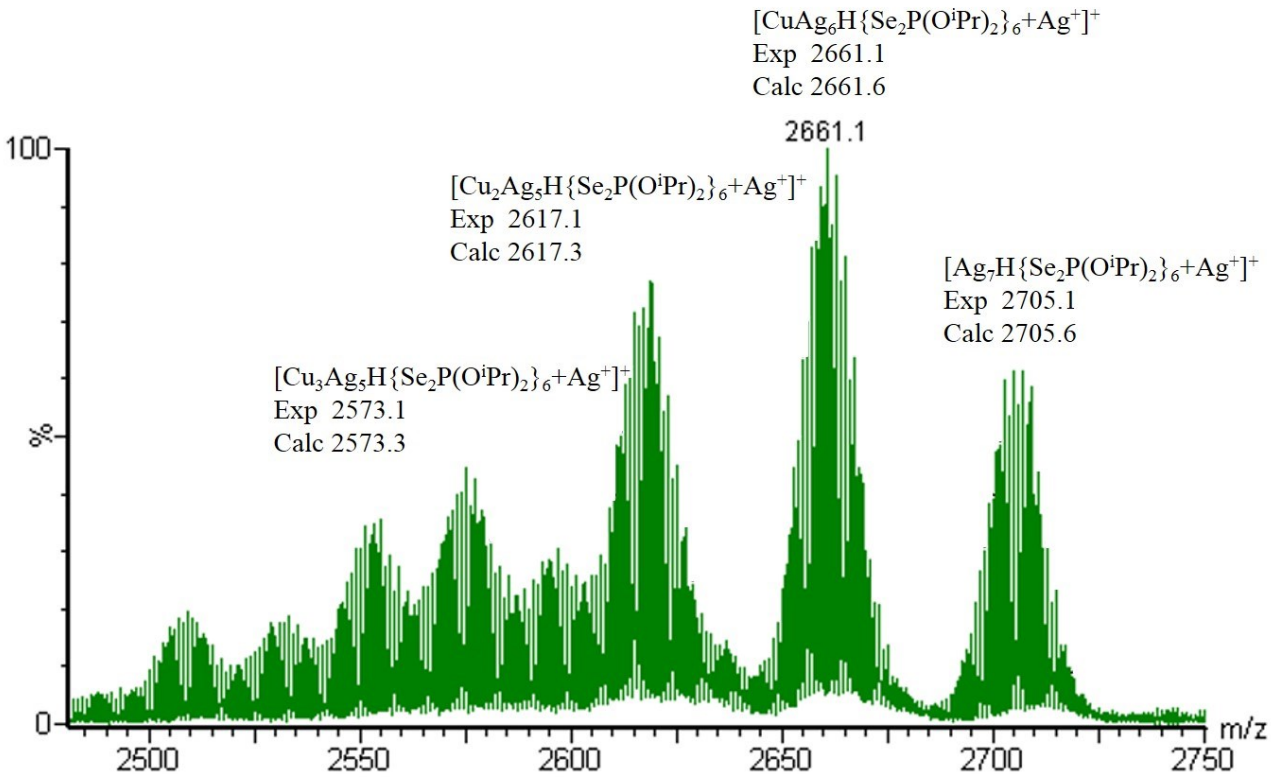

Figure S21. The positive mode of ESI mass spectrum of crystalline sample of $CuAg_6(H)\{Se_2P(O^iPr)_2\}_6$ (**6a**).

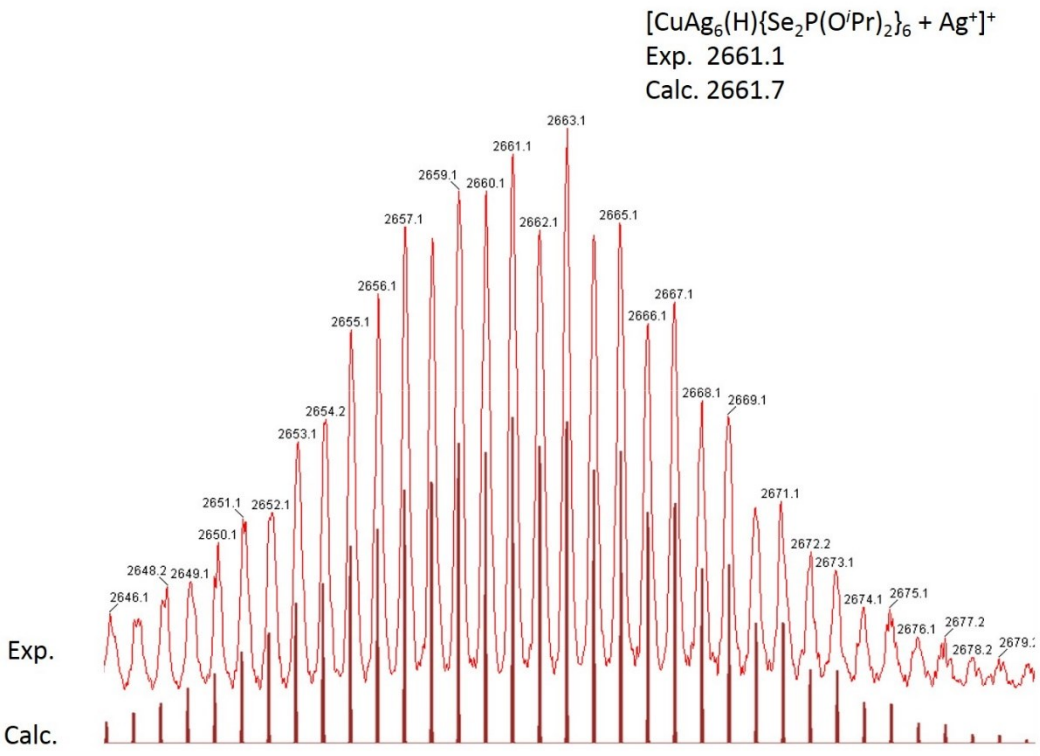

Figure S22. The experimental (top) and calculated (bottom) isotope distribution of

$[CuAg_6(H)\{Se_2P(O^iPr)_2\}_6 + Ag^+]^+$.

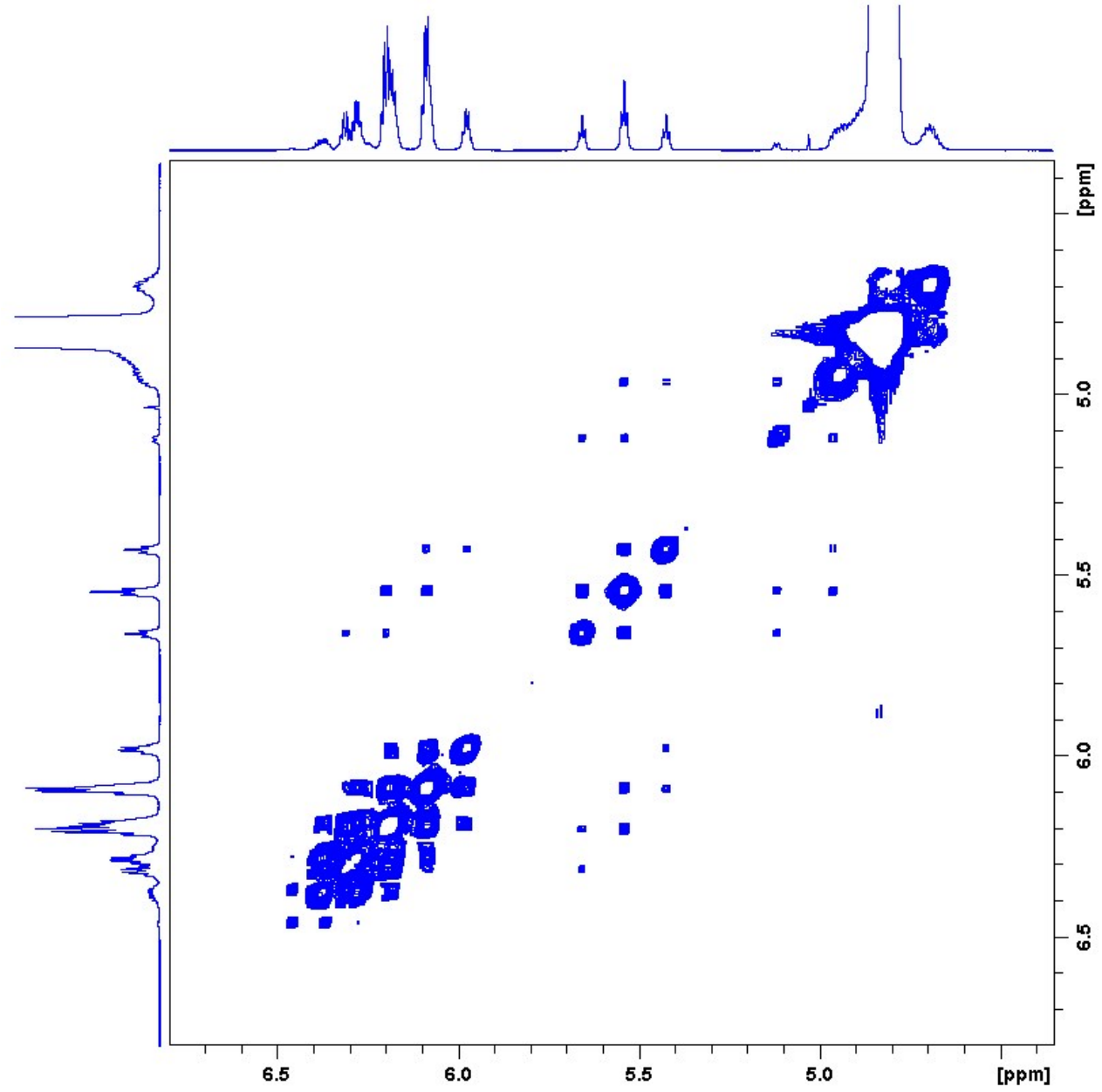

Figure S23. ^1H-^1H 2D EXSY NMR spectrum of the resulting product from the reaction of **1** and **2** with equal molar ratio.

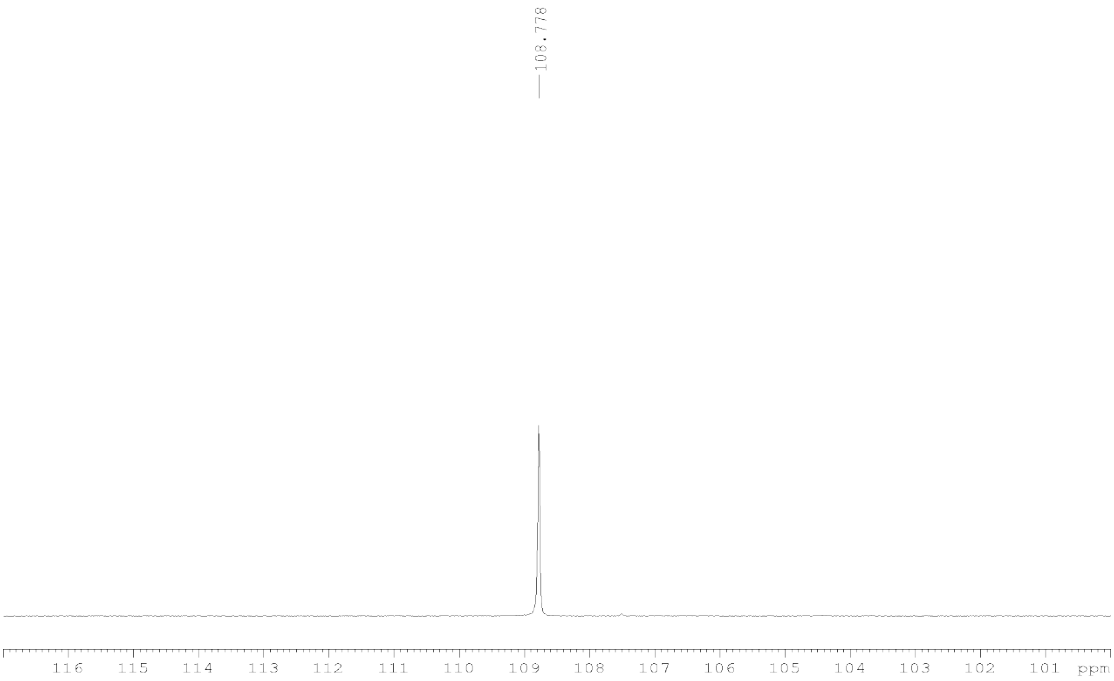

Figure S24. $^{31}P\{^{1}H\}$ NMR spectrum of $Ag_7(H)\{S_2P(O^iPr)_2\}_6$ (**1**).

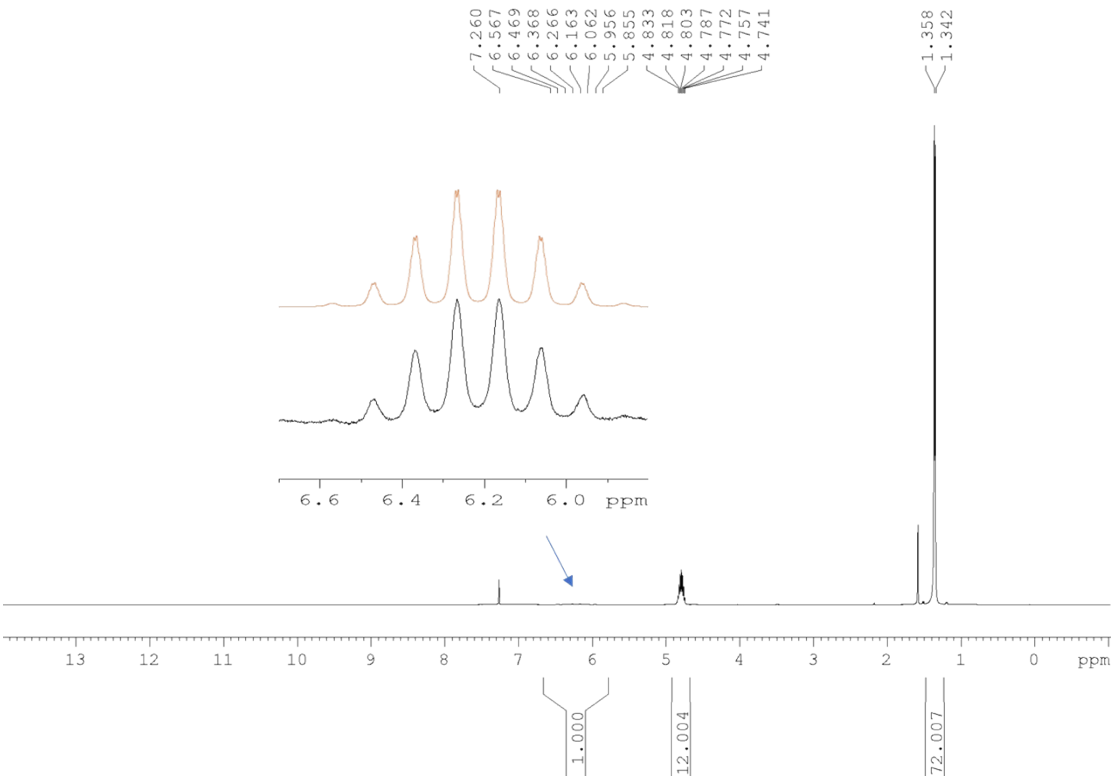

Figure S25. ^{1}H NMR spectrum of $Ag_7(H)\{S_2P(O^iPr)_2\}_6$ (**1**). Spectra in the inset are simulation (top) and experimental (bottom), respectively.

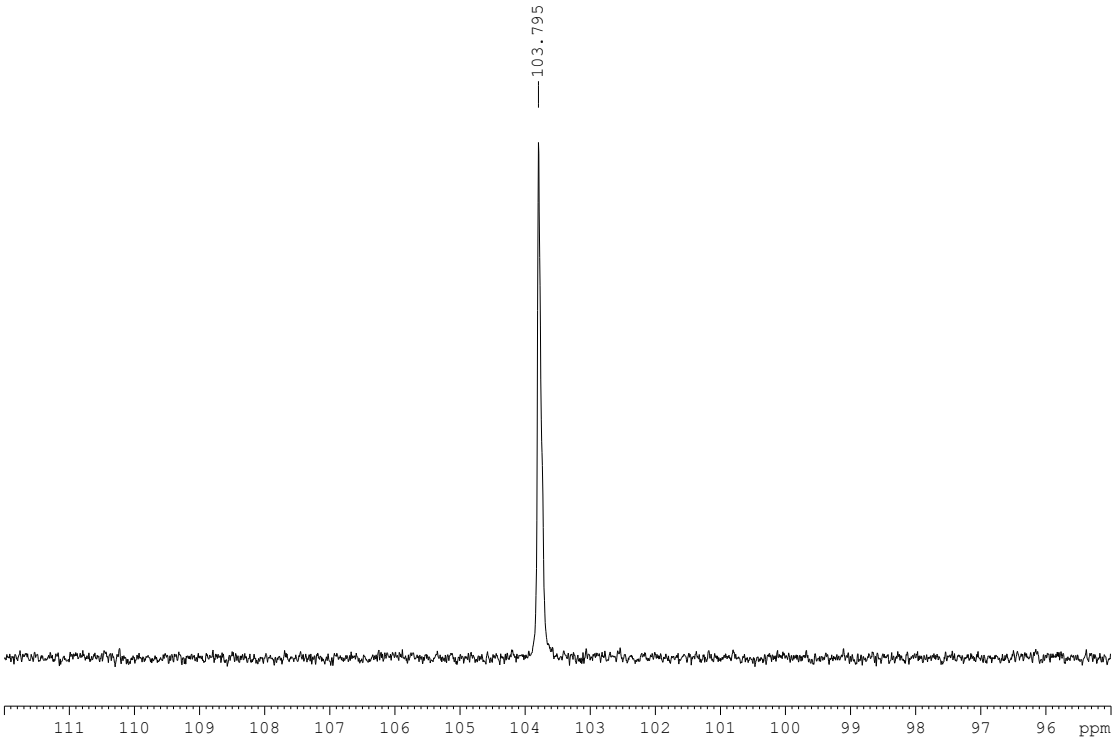

Figure S26. $^{31}P\{^{1}H\}$ NMR spectrum of $Cu_7(H)\{S_2P(O^iPr)_2\}_6$ (**2**).

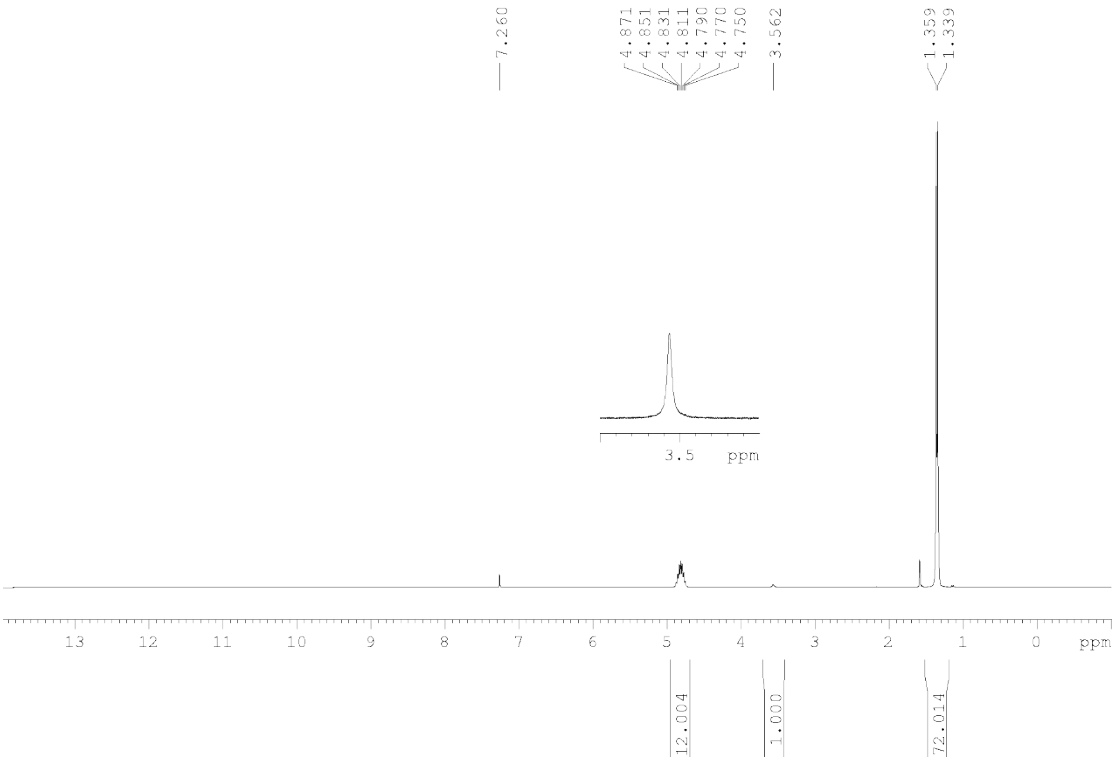

Figure S27. ^{1}H NMR spectrum of $Cu_7(H)\{S_2P(O^iPr)_2\}_6$ (**2**).

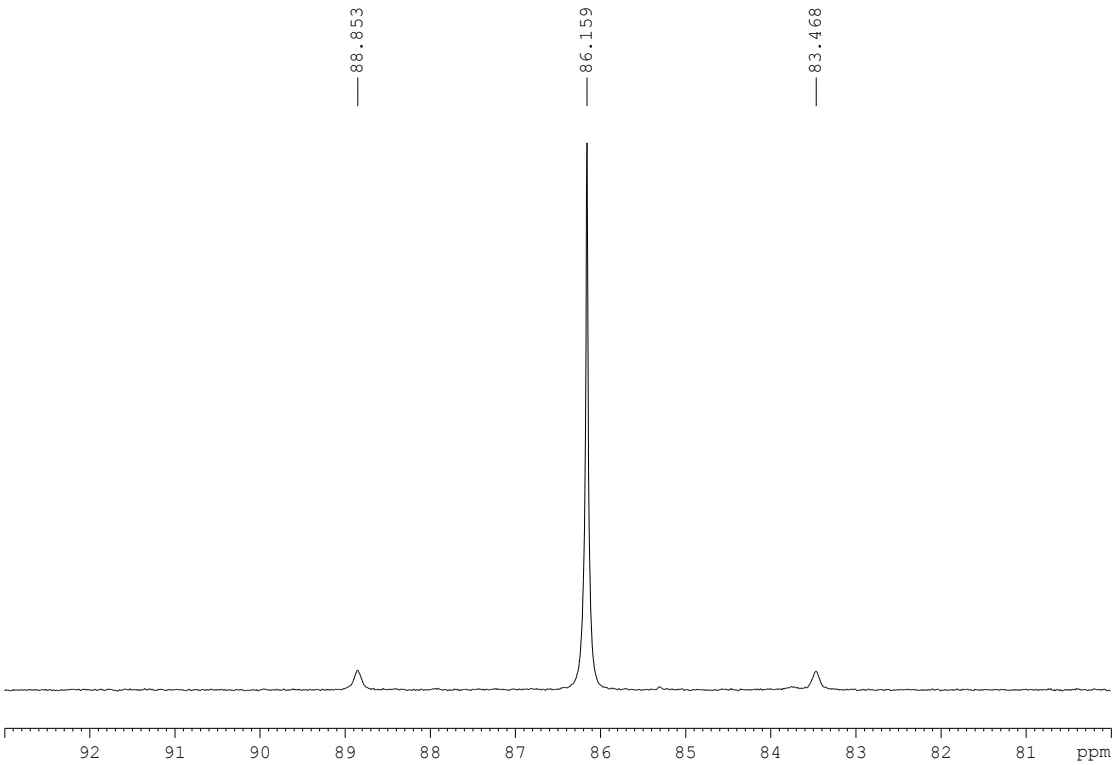

Figure S28. $^{31}P\{^{1}H\}$ NMR spectrum of $Cu_7(H)\{Se_2P(O^iPr)_2\}_6$ (**4**).

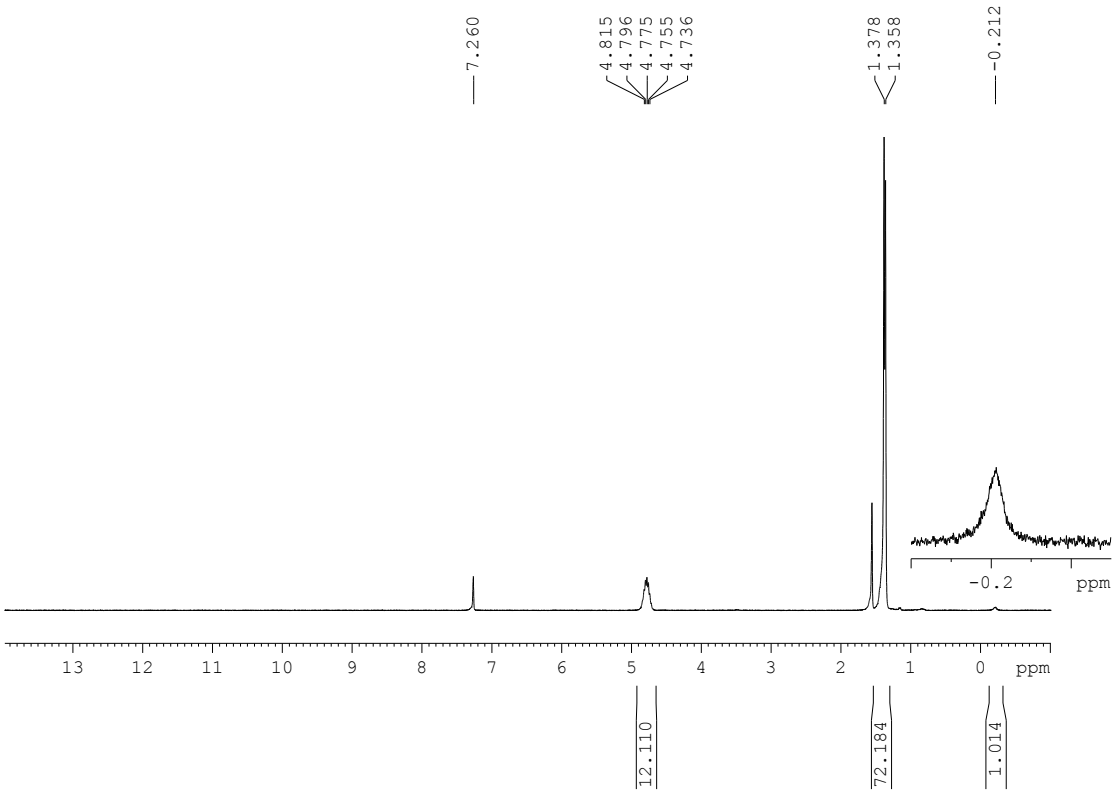

Figure S29. ^{1}H NMR spectrum of $Cu_7(H)\{Se_2P(O^iPr)_2\}_6$ (**4**).

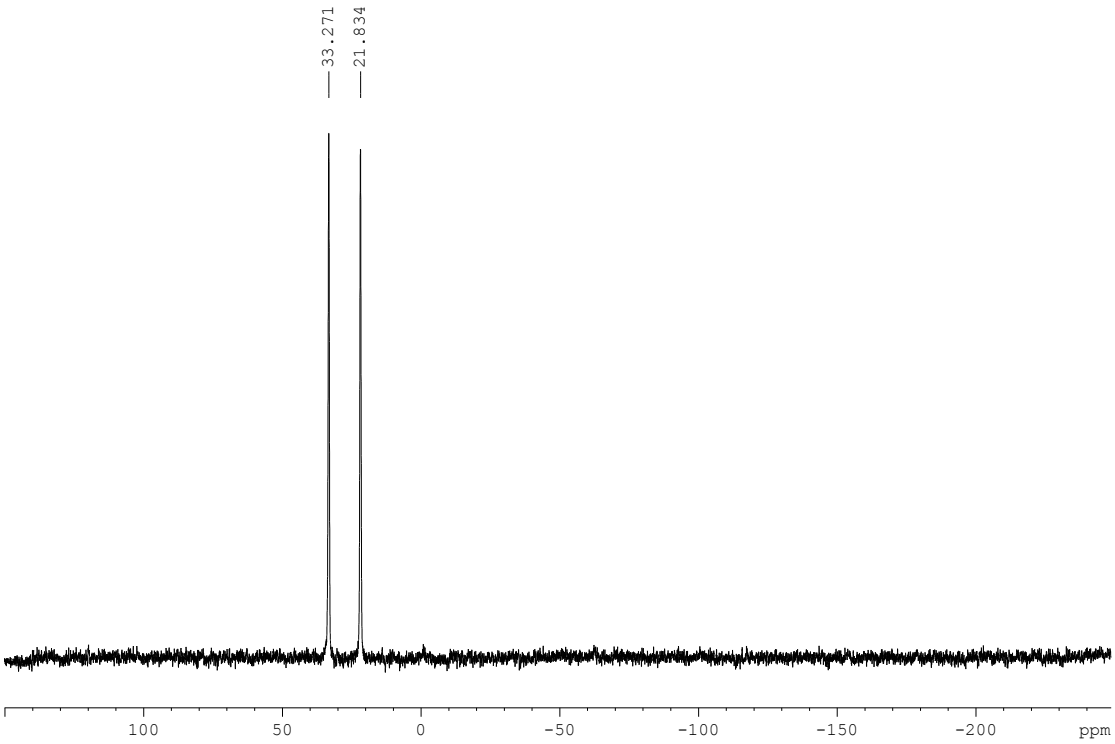

Figure S30. ^{77}Se NMR spectrum of $Cu_7(H)\{Se_2P(O^iPr)_2\}_6$ (**4**).

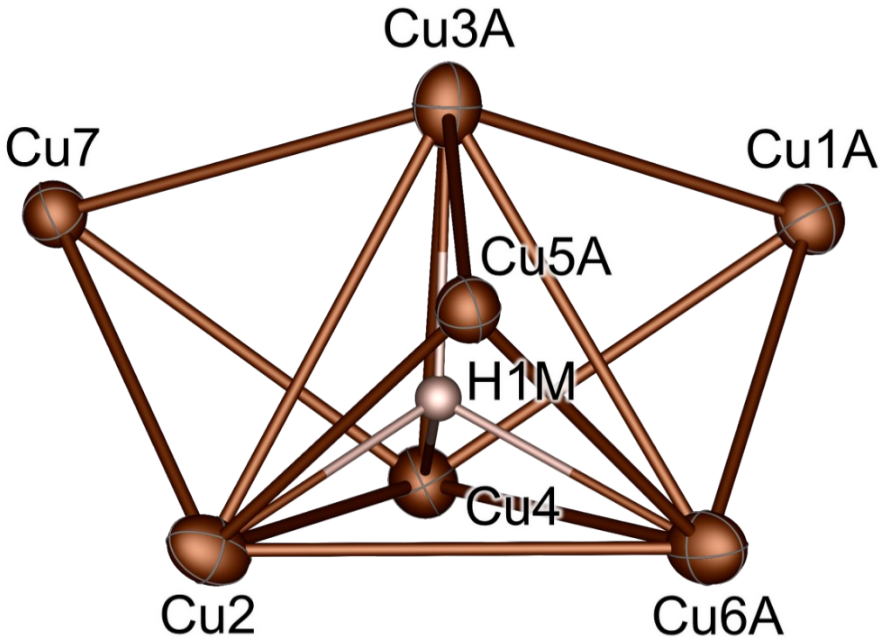

Figure S31. ORTEP drawing (50% probability) of $Cu_7(H)$ core in $Cu_7(H)\{S_2P(O^iPr)_2\}_6$ (**2**). Symmetry code: A: 2-x, 1-y, 1-z.

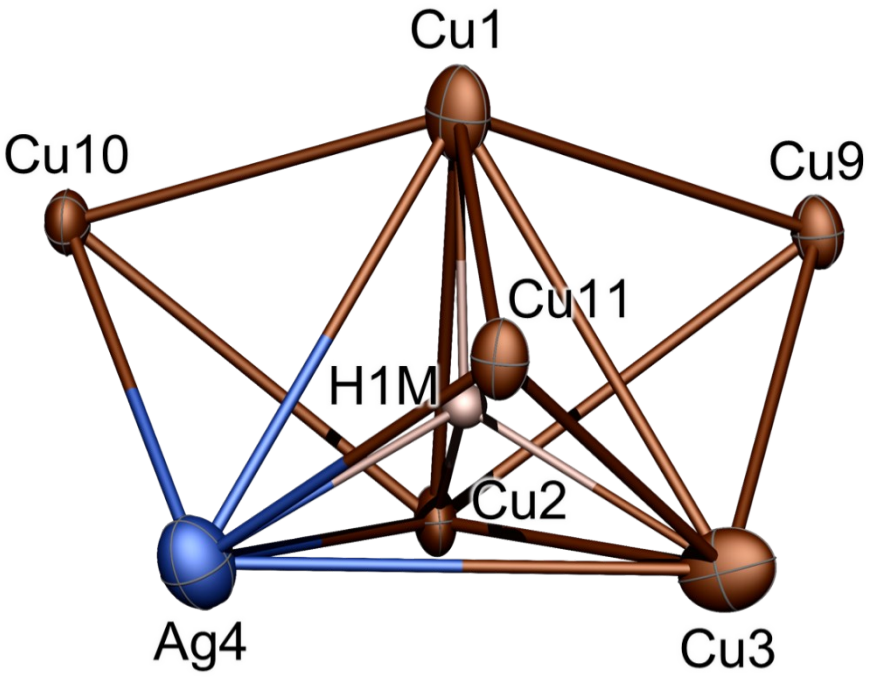

Figure S32. ORTEP drawing (30% probability) of $Cu_6Ag(H)$ core in **5**a.

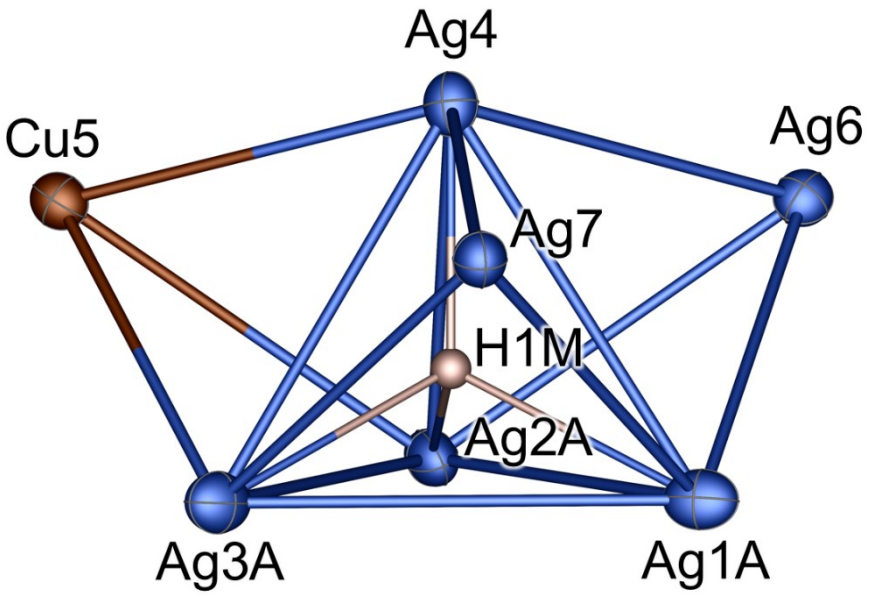

Figure S33. ORTEP drawing (50% probability) of $CuAg_6(H)$ core in $CuAg_6(H)\{Se_2P(O^iPr)_2\}_6$ (**6a**). Symmetry code: A: 1-x, 1-y, 1-z.

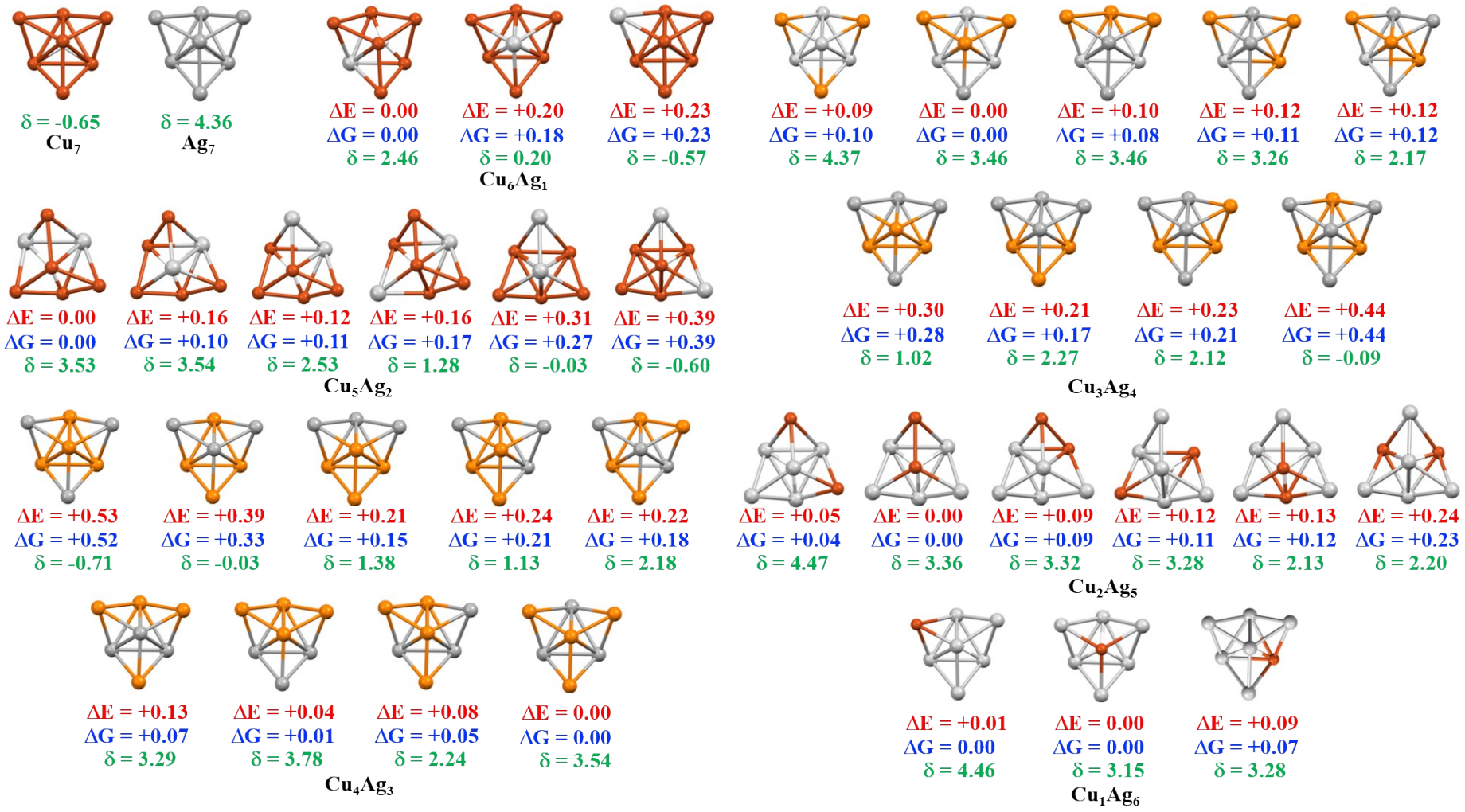

Figure S34. Core structures and relevant computed data for **3'**, **4'** and the various isomers of the heterometallic Cu_xAg_{7-x} models **6'** (ligands not represented). ΔE and ΔG are the isomer relative energies and free energies at 298 K, respectively (in eV). δ is the computed ^1H hydride chemical shift.

Table S1. Ratio of each compound in **5**. The percentage yield is calculated based on the integration of each peak in ^{31}P NMR spectra.

Cu_7:Ag_7 ratio	6 : 1	4 : 1	2 : 1	1 : 1	1 : 2	1 : 4	1 : 6
	^{31}P (%)	^{31}P (%)	^{31}P (%)	^{31}P (%)	^{31}P (%)	^{31}P (%)	^{31}P (%)
Cu_7	23.5	9.3					
Cu_6Ag_1	66.3	37.7	16.5	2.5	3.2		
Cu_5Ag_2	10.2	49.2	41.5	17.3	17.3	2.4	
Cu_4Ag_3		3.8	33.3	38.9	21.8	11.7	
Cu_3Ag_4			7.2	21.9	22.2	18.1	
Cu_2Ag_5			1.5	14.2	30.5	31.2	10.7
Cu_1Ag_6				4.7	21.8	27.9	43.6
Ag_7				0.5	5.4	8.7	45.7

Table S2. The chemical shifts and coupling constants of $Cu_xAg_{7-x}(H)\{S_2P(O^iPr)_2\}_6$ (**5**).

	^{1}H NMR			^{109}Ag NMR	
	Chemical shift (ppm)	$^1J_{1H\text{-}107Ag}$ (Hz)	$^1J_{1H\text{-}109Ag}$ (Hz)	Chemical shift (ppm)	$^1J_{1H\text{-}109Ag}$ (Hz)
Cu_7	3.56	-	-	-	-
Cu_6Ag_1	5.00	86.7	99.7	--	--
Cu_5Ag_2	5.44	65.0	74.7	1080.5	74.5
Cu_4Ag_3	6.05	62.9	72.3	1120.9	72.7
Cu_3Ag_4	6.08	57.4	66.0	1140.2	66.6
Cu_2Ag_5	6.12	52.3	60.1	1137.4	60.0
Cu_1Ag_6	6.13	44.6	51.3	--	--
Ag_7	6.22	39.4	42.6	--	--

Table S3. The chemical shifts and coupling constants of $Cu_xAg_{7-x}(D)\{Se_2P(O^iPr)_2\}_6$ ($\mathbf{6_D}$).

	Chemical shift (ppm)	**$^1J_{2H\text{-}107Ag}$ (Hz)**	**$^1J_{2H\text{-}109Ag}$ (Hz)**
Cu_7D	-0.294	-	-
Cu_6Ag_1D	1.215	10.7	12.3
Cu_5Ag_2D	1.919	8.9	10.3
Cu_4Ag_3D	2.603	8.8	10.2
Cu_3Ag_4D	2.942	8.3	9.5
Cu_2Ag_5D	3.235	7.6	8.7

Table S4. Selected crystallographic data of **2**, **5a**, and **6a**.

	2	**5a**	**6a**
Compound	$Cu_7(H)\{S_2P(O^iPr)_2\}_6$	$2[Cu_6Ag(H)\{S_2P(O^iPr)_2\}_6][Cu_7(H)\{S_2P(O^iPr)_2\}_6]$	$CuAg_6(H)\{Se_2P(O^iPr)_2\}_6$
CCDC Number	2051209	2051210	2051211
Chemical formula	$C_{36}H_{85}Cu_7O_{12}P_6S_{12}$	$C_{108}H_{255}Ag_2Cu_{19}O_{36}P_{18}S_{36}$	$C_{36}H_{85}Ag_6CuO_{12}P_6Se_{12}$
Formula weight	1725.35	5264.72	2554.14
Crystal System	Trigonal	Monoclinic	Triclinic
Space group	*R*(-)3	$P2_1/n$	*P*(-)1
a, Å	42.5764(12)	13.3391(6)	12.5584(6)
b, Å	42.5764(12)	36.3109(14)	13.4971(6)
c, Å	13.1174(5)	21.0510(9)	13.5892(7)
α, deg.	90	90	110.4600(10)
β, deg.	90	93.3921(13)	98.1499(5)
γ, deg.	120	90	109.9450(10)
V, Å^3	20592.8(14)	10178.3(7)	1816.87(15)
Z	12	2	1
Temperature, K	100(2)	100(2)	100(2)
ρ_{calcd}, g/cm^3	1.670	1.718	2.334
μ, mm^{-1}	2.678	2.693	8.057
θ_{max}, deg.	24.999	25.000	27.182
Completeness, %	100.0	99.9	98.6
Reflection collected / unique	45406 / 8061 [R_{int} = 0.0388]	81366 / 17887 [R_{int} = 0.0410]	16325 / 7859 [R_{int} = 0.0399]
Restraints / parameters	187 / 536	360 / 1146	108 / 374
[a]*R*1, [b]*wR*2 [I > 2σ(I)]	0.0379, 0.0905	0.0721, 0.1845	0.0347, 0.0701
[a]*R*1, [b]*wR*2 (all data)	0.0474, 0.0971	0.0872, 0.1971	0.0487, 0.0759
GOF	1.022	1.028	1.024
Largest diff. peak and hole, e/Å^3	1.772 and -0.831	2.487 and -1.259	0.977 and -0.689

[a] $R1 = \Sigma \mid \Box F_o \Box - \Box Fc \Box \mid / \Sigma \Box F_o \Box$. [b] $wR2 = \{\Sigma[w(F_o^2 - F_c^2)^2]/\Sigma[w(F_o^2)^2]\}^{1/2}$.

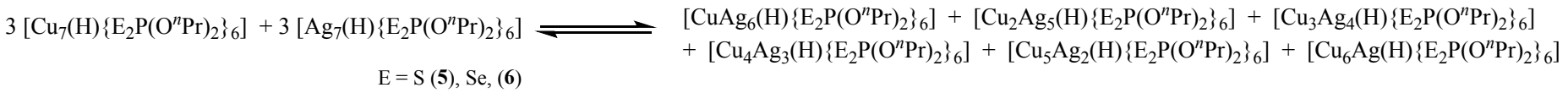

Scheme S1. The equation of the inter-cluster reactions.

$$K_c = \frac{[CuAg_6(H)\{E_2P(O^nPr)_2\}_6]\,[Cu_2Ag_5(H)\{E_2P(O^nPr)_2\}_6]\,[Cu_3Ag_4(H)\{E_2P(O^nPr)_2\}_6]\,[Cu_4Ag_3(H)\{E_2P(O^nPr)_2\}_6]\,[Cu_5Ag_2(H)\{E_2P(O^nPr)_2\}_6]\,[Cu_6Ag(H)\{E_2P(O^nPr)_2\}_6]}{[Cu_7(H)\{E_2P(O^nPr)_2\}_6]^3\,[Ag_7(H)\{E_2P(O^nPr)_2\}_6]^3}$$

E = S (**5**), Se, (**6**)

Scheme S2. The expression of equilibrium constant based on the scheme 1.